Calling the Cedar River's Bluff: A study of bed elevation changes and characterizing bluff grain size distributions in the Cedar River upstream of a depositional zone in the City of Renton, Washington

Written By

Hannah Karlsson

A report prepared in partial fulfillment
of the requirements for the degree of
Master of Science
Earth and Space Sciences:
Applied Geosciences University of Washington

March 2019

Reading committee:
Brian Collins
Dan Scott

MESSAGe Technical Report Number: 073

EXECUTIVE SUMMARY

The Cedar River, a 477 km^2 basin draining the Western Cascade Range, has experienced meters of channel aggradation over the last century in the lower three river kilometers (rkm), which has reduced channel conveyance and increased flooding hazards in Renton, Washington. To understand potential drivers of the channel aggradation in Renton this study investigates potential sediment supply from upstream bed incision over the last 18 years and the proportion of sediment delivered from a channel-marginal bluff that has the potential to contribute to the aggrading bed in Renton. In 1916 the Masonry Dam was constructed, which reduced flows and impounded sediment upstream, possibly causing downstream channel incision. In the 1960's, levees and revetments were constructed along 60% of the lower 36 kilometers of the Cedar River banks. A gravel supply study in 2002 suggests that channel incision occurred following flow reduction from the dam and the construction of the levees and assisted in preventing the river from flooding the width of the valley floodplain (Perkins et al., 2002). Previous studies have assessed bed elevation changes in the first 35 rkm of the Cedar River between 2000 and 2012. The first objective of this study analyzes bed elevation over the last 18 years to identify whether channel incision is a potential sediment source for the aggrading bed in Renton. Additionally, it analyses cross sections within recent levee setback projects and a landslide zone that have changed the shape of the channel.

By comparing existing cross-sectional data from 2000 and 2003 to 2012 and 2012 to 2018, this study reveals there has been no net change in bed elevation. Therefore, bed incision has not contributed to the aggradation in Renton over the last 18 years. During this time, a landslide in 2001 and two levee setback projects altered the active channel and opened the river back to its floodplain. Although these alterations to the channel have higher variability in bed elevation

changes, no net average elevation changes were detected. The 2001 landslide between rkm 7.7 and 8.3 has an average cross section change in bed elevation of 0.02 m/yr with a standard error of (±) 0.00 m/yr from 2000 to 2012 and -0.04 ± 0.04 m/yr from 2012 to 2018 (number of cross sections (n) =6). The Cedar River Rapids levee setback between rkm 11.5 and 11.9 has an average bed elevation change of -0.01 ± 0.02 m/yr from 2000 to 2012 right after it was constructed in 2012 and -0.00 ± 0.03 m/yr from 2012 to 2018 (n=4). Rainbow Bend, the second levee setback zone upstream, constructed in 2014 at rkm 17.2 to 18.5, has an average elevation change of 0.02 ± 0.04 m/yr between 2012 and 2018 (n=9). All sub-reaches are not statistically different from a zero net elevation change using a two-tailed t-test at a confidence level of 95%.

The second objective of this study is to estimate the grain size distribution of a bluff previously estimated to have the largest sediment supply to the lower Cedar River and evaluate the proportion of grain sizes in the eroding bluff contributing to channel aggradation in Renton. Perkins et al. (2002) reported that 49% of the sediment supplied to the lower Cedar River is from bluff retreat and visually estimated the proportion of gravel in each contributing bluff. This study tests a grain size image detection method to obtain a more accurate estimate of the bluff grain size distribution than the previous visual estimates. Based on the resolution of the images collected in the field, the optical granulometry methodology used in this study was determined to confidently detect particle sizes larger than approximately 95 mm and therefore failed to give a more accurate measurement of the smaller gravel distributions in the bluff. Smaller grain sizes were measured using grab sample sieve analysis and facies mapping of sand lenses in the bluff, estimating 21% sand in the bluff. The sand lenses mapped in the images gave a relatively objective measurement of the minimum proportion of sand in the bluff from sand lens deposits than visual estimates. The grab sample grain sizes, although not representative of the entire bluff,

reveal a total sand proportion 16% higher proportion of sand than previous estimated. The bluff estimates are compared to existing bed material samples in Renton. The estimated bluff gravel proportion, after assuming a fourth of the material is lost to attrition, contributes approximately 60% to the gravel to the upper 2.5 to 2 rkm in Renton. The sand proportions of the bluff contribute to the lower reaches in Renton. Therefore, the bluff is an important source of sediment depositing in Renton and to the associated increase in flood frequency.

TABLE OF CONTENTS

LIST OF FIGURES

LIST OF TABLES

ACKNOWLEDGMENTS

Thank you to King County and Northwest Hydraulic Consultants for all the support and data that was provided for this study. I could not have done it without the massive inventory of information that has been collected on the Cedar River over the years. Thank you to Dan Scott who facilitated field work and piloted the drone along the Cedar River. Thank you also to Brian Collins and Dan Scott for the incredibly valuable knowledge and experience on rivers in the Pacific Northwest.

INTRODUCTION

The Cedar River, which drains 477 km^2 of the western Cascade Range (Fig. 1), has experienced meters of sediment accumulation in the first three river kilometers (rkm) in the Renton, Washington before reaching Lake Washington. Stage-discharge field measurements for the USGS stream gaging station in Renton (No. 12119000) show approximately 2.2 meters of aggradation from 1945 to 2012 (Gendaszek et al., 2012). The increase in channel bed elevation has contributed to an increase in flood frequency in the developed City of Renton (U.S. Army Corps of Engineers (USCOE), 1997). Consequently, the City of Renton has resorted to dredging the first 2.5 rkm of the Cedar River to increase flood capacity. The dredging provided 100-yr flood protection for the first 1.6 rkm of the Cedar River within the City of Renton. In 1998 and 2016 the USCOE dredged the channel bed to a depth of 1.8 to 2.4 and 1 to 1.6 meters respectively (NHC, 2001; NHC, 2017). Northwest Hydraulic Consultant Inc. (NHC) was contracted by the City of Renton to monitor sediment accumulation in the last 3.3 rkm of Renton on a yearly basis since the 1998 dredging project.

Where is all this sediment coming from upstream? A gravel study in 2002 reported 49% of upstream gravel sources came primarily from bluff retreat, and suggested a potential for channel bed incision upstream. A previous comparisons of cross section data between 2000 and 2012 from Landsburg to upstream of Renton revealed wide variability in bed elevation (King Country, 2015). This study expands upon the understanding of two potential sediment drivers causing sediment accumulation in Renton by investigating (1) bed incision over the last 18 years along the Cedar River and within recently altered sections of the channels around levee setbacks and landslides, (2) a grain size distribution of a known bluff sediment source, using optical

granulometry, previously estimated by Perkins et al. (2002). Bluff grain size proportions are compared with existing bed material samples in Renton to understand the potential for bluff sediment to contribute to aggradation in Renton.

Sediment supply for the lower Cedar River comes from a contributing area of 285 km^2 below the Masonry Dam, constructed in 1916, which reduced flows and retained sediment upstream of the dam (King County, 1993). The Landsburg Diversion was built 19.3 rkm downstream of the Masonry Dam and diverts water from the Cedar River. A common response to channel impoundment is degradation directly downstream of the dam (Williams and Wolman 1984). Typically, bed degradation occurs over the first several decades of dam closure. Over time the degradation decreases, and the channel adjusts to a new stable channel, usually in part due to a coarsening of the bed material (Williams and Wolman 1984; Grant 2012). The USGS gaging station (No.12117500), 0.8 rkm downstream of Landsburg Diversion, shows no net changes in bed elevation since the 1920's (Gendaszek et al., 2012). In the 1960's, approximately 60% of the lower 36 km of the Cedar River's banks were armored with revetments and levees (Gendaszek et al., 2012; King County 2015). The first objective of this study is to investigate changes in channel bed elevations in the lower 36 rkm of the Cedar River over the last 18-years by using cross sectional data from 2000, 2003, 2012 and 2018. Additionally, spatial analysis is conducted where the channel shape abruptly changed from two levee setback projects and a landslide in the last 18 years. A decrease in channel bed elevation upstream of Renton would suggest channel incision below the Landsburg gaging station is potentially contributing to the channel aggradation in Renton.

Another possible driver of channel aggradation in Renton is the volume and caliber of eroding channel-marginal bluff sediment sources upstream. Perkins et al. (2002) calculated 49% of the

gravel supplied to the Cedar River below Landsburg is from bluffs by measuring bluff retreat from 1936 to 2000. The second objective of this study is to test optical granulometry methods to characterize the grain sizes of a large channel-marginal bluff and compare them to grain size distributions of existing bed material in Renton to estimate how much of the bluff material is potentially contributing to the Renton Reach. The bluff selected to be characterized in this study was estimated to supply the largest amount of gravel to the lower Cedar River (Perkins et al., 2002). Perkins et al. (2002) visually estimated that the bluff, located at rkm 33.4, contains 95% gravel, and had a retreat rate of approximately 19 cm/yr from 1936 to 1999. This estimation of bluff retreat and gravel proportions motivates the application of an optical granulometry method to obtain a more accurate estimate of the cumulative grain size distributions of the entire bluff.

BACKGROUND

Study Area

The Cedar River basin is sectioned by three different water management authorities. The upper and middle Cedar River basin–between the headwaters in the Cascade Range to the Chester Morse Reservoir retained by the Masonry Dam at rkm 54.5 and downstream to the Landsburg Diversion at rkm 35.2–is managed by the Seattle Public Utilities municipal water supply (King County, 1993). The lower Cedar River basin–32 km of river between the Landsburg Diversion to Lake Washington–is a mix of developed and undeveloped land managed by the King County Water and Land Resources Division. The last 3 rkm of the Cedar River–where most deposition has occurred–is managed by the City of Renton. The main study area for this project is between Landsburg at rkm 35.2 and the City of Renton at ~3.3 rkm (Fig. 1).

Geologic Setting

The last glaciation by the Puget Lobe of the Cordilleran Ice Sheet extended into the Puget Lowlands 16,950 years ago (Porter & Swanson, 1998). At the end of the Pleistocene 16.5 cal. ka BP the Cordilleran Ice Sheet retreated north from the Puget Lowland leaving hundreds of meters of glacial deposits comprised of discontinuous sequences of advance outwash, till, glaciolacustrine, and recessional outwash material (Mullineaux, 1970; Booth, 1994) (Fig. 2). The Cedar River drains the Cascades from east to west and incised the glacial deposits after deglaciation (Collins and Montgomery, 2011). The lower Cedar River formed a wide (~0.5 km) valley floor composed of sand and gravel alluvium (Booth, 1995). The gradient of the lower Cedar River decreases from 0.007 near Landsburg to 0.003 above the Renton depositional zone (Perkins et al. 2002).

The lower Cedar River meanders at the base of the incised post-glacial valley and has steep glacial outwash bluffs (Booth, 1994) that experience extensive mass wasting and bluff retreat (Perkins et al., 2002) (Fig. 2). The majority of the tall contributing bluffs, composed of glacial outwash deposits, are between Landsburg and rkm 28 along the lower Cedar River (Perkins et al., 2002) (Fig. 2). The contributing bluff characterized in this study is a recessional outwash bluff composed of well-sorted gravels and sands with discontinuous sand lens deposits (Booth, 1995) (Fig. 2).

Channel alterations over the last century

Prior to 1912, the Cedar River flowed west into the Black River, which was the southernmost outlet for Lake Washington (Chrzastowski, 1986). During this time, when the Cedar was at flood stage, flows extended northward through floodplains and wetlands and directly into Lake Washington (Eastwick, 1891). When the Lake Washington Ship Canal was built in 1916, the lake lowered by ~3 m (Chrzastowski, 1986), the Black River dried up, and the Cedar River was rerouted by a straight engineered channel into Lake Washington. The engineered channel is where most of the deposition has occurred in the Cedar River and is the main area of concern for flooding due to bed aggradation.

In the last century, the Cedar River has undergone extensive anthropogenic modification from dams and bank armoring in the lower 36 kilometers, which have reduced flows and sediment supply. Since the Masonry Dam was built, the flows have decreased the 2-, 10-, and 100-year recurrence interval by 47%, 54% and 56%, respectively (Gendaszek et al., 2012) and retained all coarse sediment supply upstream of the dam. The Landsburg Diversion retains sediment supply to the lower Cedar River at low flows but flushes sediment through its gates at flows exceeding a 1 to 1.2 -year recurrence interval (~28 to 42 m^3/s; Inter-Fluve, Inc., 2000). The lower Cedar

River has transformed from a wide anastomosing channel with an average channel width of 47 meters in 1936 to a narrow single channel river with a width of 23 meters in 1989 (Gendaszek et al., 2012).

There have been several major alterations to the Cedar River in the last 18 years. In the recent decade, King County has implemented levee setback projects to open the floodplain back to the river channel (Table 1). Levee setback projects along with high flow events in 2009 and 2011 have increased the average channel width to approximately 34 meters (Gendaszek et al., 2012). In this study, average bed elevation changes are sectioned into sub-reaches for two major levee setback areas: Cedar River Rapids project constructed in 2012 from rkm 11.5 to 11.9 and Rainbow Bend project constructed in 2014 from rkm 17.2 to 18.5. Another major alteration to the Cedar River in the last 18 years was a landslide event triggered by a 6.8 magnitude earthquake on February 28, 2001 (Highland, 2002). The landslide activated on the right bank of the Cedar River at rkm 8, deposited 38,000 cubic meters of glacial deposits into the Cedar River Valley, and rerouted the river channel to the south (Highland, 2002). The conveyance capacity from 2000 to 2003 was constant despite the large volume of sediment that deposited in the reach from the landslide (Timm and Wissmar 2013). This study uses sub-reaches within the cross-sectional data to assess localized channel bed elevation changes within levee setback and the landslide.

Optical granulometry

Over the last 20 years, several groups have derived surface grain-size distribution of fluvial sediment from digital images (McEwan et al., 2000; Butler et al., 2001; Sime and Ferguson, 2003). BASEGRAIN is a grain size detection software developed by Detert and Weitbrecht (2012), implementing MATLAB image analysis code and object detection functions. The

BASEGRAIN software is used in this study because of its user-friendly platform and ability to manually correct grain sizes that are inaccurately detected. The software was originally developed to digitally measure grain sizes in gravel bedded rivers using aerial images of the river bed. This study implements the digital image grain size detection method and tests its feasibility to gather more accurate estimates of bluff grain size distributions than previous methods of visual inspection used by Perkins et al (2002).

METHODS

Cross Section Survey Comparison

This study calculated changes in channel bed elevation using existing surveyed cross-sectional data from 2000, 2003, 2012, and Light Detection and Ranging (LiDAR) and bathymetric surveys from 2018. All survey coordinates were referenced to NAD 1983 datum HARN State Plane Washington North coordinate system. In 2000 and 2003, the Cedar River Flood Insurance Study established over two hundred cross sections along the lower Cedar River (Federal Emergency Management Agency, 2005). In 2012, 204 of the cross sections from rkm 3 to 36 were resurveyed by contractors, Minister & Glaeser Surveying, retained by King County. The flood study surveys and 2012 King County surveys were provided as distance and elevation data with georeferenced linear shapefiles along the survey points (Fred Lott, email communication, 2018). Most recently, in 2018 King County obtained one meter-resolution LiDAR/bathymetry surveys along the lower Cedar River. The elevation profiles of the LiDAR/bathymetry along the 2012 linear shapefile coordinates are interpreted to create the 2018 cross sections (Appendix A). To simplify nomenclature, the comparison of the survey data from 2000 and 2003 to 2012 is referred to as 'the earlier survey period' and the comparison from 2012 to 2018 surveys is referred to as 'the later survey period' for the following sections of this report.

The average elevations of the channel bed for all cross sections were calculated in this study using similar methods to those performed by NHC in the Renton reach cross-sections in order for this study's measurements to be comparable to NHC's measurements (NHC, 2001). The extent of the active channel for each cross section was determined by choosing points of similar elevation on the left and right channel banks at bankfull using the cross-sectional shape. Aerial

imagery from the same years as the surveys were utilized to delineate the active channel in the cross sections by marking transitions from active bars to the vegetated edges of banks along each cross section. In confined areas of the channel, with revetments and levees on either side, the base of each structure was determined to be the extent of the active channel bed. This is predominantly the case in the Renton Reach, where levees confine both sides of the channel.

Excel and R software was employed to calculate the average bed elevations of all cross sections collected between rkm 3 to 36. A weighted average channel elevation for each cross section was calculated by the sum of the average survey elevations between adjacent survey points multiplied by the distance between the adjacent points within the chosen extent of the active channel. The sum of the areas was then divided by the cross-sectional width of the channel bed to produce a weighted average elevation of the channel bed from the survey points (e.g. Prych, 1988). The change in average channel elevations between survey years for each cross section was computed by taking the difference in each average channel elevation between 2000 and 2012 or 2003 and 2012 as the earlier survey period and between 2012 and 2018 as the later survey period. Yearly rates of positive (depositional) and negative (incisional) changes were calculated by dividing the total change in bed elevation by the number of years between cross sectional surveys. Once the changes in average bed elevations between the survey periods for all cross sections were calculated, a weighted mean of the average cross section elevation changes based on the distance between each survey cross section along the river was derived to determine the net change in bed elevation throughout the study area. The two levee setback projects and the 2001 landslide zone were separated into sub-reaches and the change in elevations for the cross sections within the sub-reaches were averaged to determine a localized net elevation charge. In order to determine

variability in the calculated bed elevation averages, a standard error of all average elevations was calculated.

A two-tailed t-test was applied to the averaged net elevation change of the entire study area and sub-reaches to statistically distinguish net changes in elevations from no change in channel elevations at a 95% confidence level. The null hypothesis states that no net change is detected, and the alternative hypothesis states a net position or negative change in elevation is detected.

The sources of error and variability in comparing the survey years were related to the survey point spacing in survey data and determining appropriate extents of the active channel bed to compute average bed elevation. The density of survey points is much greater in the 2012 and 2018 surveys than in the 2000 and 2003 surveys. The steep banks and bluff sections of the surveys were also subject to increased errors in the LiDAR and land survey accuracy due to point spacing and accessibility. Because of this, levee slopes and steep bluffs were omitted from the active channel elevations calculations. Active channel left and right extent points were selected to match up as closely as possible between survey years without excluding the change in channel width within the active channel.

Bluff Sediment Sources

The optical granulometry method was tested by collecting orthogonal photographs, a grab sample, and mapping facies on the bluff face. Images were obtained of the bluff at rkm 33.4, with a maximum height of 34 m and a length of ~250 m, on a float trip in January 2019 using a drone and hand-held cameras (Fig. 3). A 30.5 mm ruler and a 32.8 mm long rock hammer was placed on the bluff near its base as scaling tools to calibrate the resolution of the images during the processing stage. Two parallel lasers mounted a known distance apart were also brought into

the field to use as a scale. However, the low power in one of the lasers made it difficult to see both lasers on the bluff face, therefore the lasers were not used for data collection. Using the drone, orthogonal images were taken in a grid pattern along a 70-meter lengthwise section of the bluff from the water surface to the top of the bluff. Close-up images were taken of the hammer and ruler on the lower bluff at the water's edge using hand-held cameras. A 3.5 kg grab sample was collected between the ruler and hammer on the bluff. An ASTM standard sieving analysis (ASTM C136/C136M-14) was performed on the sample to measure fine grain proportions that were not expected to be detected by digital grain size analysis. Due to high flows and the difficulty of collecting samples in the field, only one grab sample was collected. To supplement the grab sample sediment distribution measurements, the sand lens facies were mapped within the bluff face (Fig. 4) and estimated the proportion of the bluff comprised solely of sand and finer sediment. Several rock falls originating from the upper bluff were observed during the two and a half hours on site at the bluff location, which demonstrates that the bluff was actively contributing sediment to the river.

All images of the bluff were processed into a DEM and orthomosaic using Pix4d software. An orthoplane was made by orienting the orthomosaic image as parallel as possible to the vertical face of the bluff. The orthoplane image of the bluff face was then analyzed using the grain size detection software, BASEGRAIN (Fig. 5). The software measures individual particle edge size and shape in the image based on the longest axis (a axis) and the perpendicular intermediate axis (b axis). A quasi-grain size distribution of the image is derived by a line-sampling methodology from the axis measurements (Fehr, 1987).

Seven subsections of the bluff with varying resolutions were used to test the accuracy of the grain size detection software and ultimately estimate a representative grain size distribution of

the eroding bluff. Two ten-by-thirty-meter areas of the orthoplane image with minimal vegetation or debris cover were analyzed in BASEGRAIN (Fig. 5). Area A includes the ruler for scale, and area B includes the hammer. To account for the vertical variability in gravel and sand lenses in the bluff deposits, images were processed from the upper and lower portion of the bluff in each of areas A and B. Additionally, grain size distributions for the individual, non-orthorectified drone images of the ruler (Drone A) and hammer (Drone B) in the lower sections of the bluff were processed. Close-up, high-resolution images taken by a hand-held camera of the ruler were also processed to determine a range of detection based on resolutions (Table 2).

To process each image in the BASEGRAIN software, the hammer and ruler scales were used to calculate a millimeter per pixel (mm/px) resolution for each image. All images were processed using the default detection parameters in the software (Detert & Weitbrecht 2013). Using these settings, Graham et al., (2005) recommends the smallest detectable grain size area should be comprised of 23 px (Table 2). Post processing tools allow the user to remove and correct visible errors in a and b axis grain detection (Fig. 6). A smaller pixel threshold was tested, however, due to the image resolution and the clasts edges being obscured by fine grain debris, post-processing could not effectively correct for detection errors in smaller pixel sizes. The minimum detectable pixel resolution was kept at 23 pixels.

The measured grain size distributions of the bluff images were limited by debris and vegetation that obscured the in-situ bluff face particles, the amount of post-processing that was done on each analyzed image, and the resolution of the collected images. Debris and vegetation cover made processing grain sizes of the entire bluff difficult. The upper section of the bluff had trees and roots that obscured the grain shapes. Debris accumulated on parts of the bluff that were not vertical or over-hanging and covered the particles within the bluff by a fine layer of sand. Due to

the time constrain of this study, post-processing was kept to a minimum by only omitting sand lenses and other fine-grained cohesive layers that are inaccurately detected in BASEGRAIN (Fig. 6). Resolution of both the drone and hand-held images influenced how grains were detected in the software, resulting in measurement errors of particle sizes during image processing. Lower resolution images caused an initial overestimate of grain sizes for the bluff by merging fine grain sections on the image to show a coarser distribution. The two hand-held images with the highest resolution detected smaller grain sizes than were present by measuring shadows, individual mineral grains in the granite clasts, and partially wetted texture in the cobbles (Fig. 7). BASEGRAIN allows for these errors to be reduced during post-processing. However, due to the limited spatial variability compared to the orthoplane image analysis and minimal post-processing, the hand-held images were not used in the average detectable grain size distributions for the bluff.

To determine an estimated grain size distribution of the spatially variable bluff deposits, optical granulometry, the finer portion of the grain size distribution from the sieved grab sample, and the sand lens proportions were used. The smallest detectable grain size for the images is calculated by multiplying the resolution of the image by Graham's (2005) truncation threshold of 23 px (Table 3). The drone image distribution proportions in areas A and B larger than the detectable particle size were averaged and used to estimate the proportion of particles larger than the detectable threshold in the bluff. The grab sample distribution was combined with the measured proportion of sand lenses from facies mapping to obtain a distribution of grain sizes smaller than the threshold grain size for the average image analysis (Fig. 11). The combined grab sample and sand lens distribution proportions were scaled to the average proportion of particles measured

from the digital grain analysis to provide an estimate of the cumulative grain size distribution of the entire bluff.

Subsurface grain sizes in the Renton reach were compiled and compared to the estimated bluff distributions. Four subsurface samples were collected on point or lateral bars in the Renton reach between rkm 0.4 to 2 by King County (1993). The size of the subsurface samples of the gravel bars were 0.1 to 0.2 cubic meters with the sample size increasing with material coarseness (Perkins et al., 2002). The USCOE collected nine subsurface samples using a McNeil core sampler from rkm 2.5 to 0.4 (Goetz, 1994). All samples were taken in close proximity to a surveyed cross section in the channel or on adjacent bars. The grain size distributions were compiled by Jones and Stokes (2002) and provided by Perkins et al. (2002). The estimated bluff grain size distributions were compared to all grain size parameters and distributions from the subsurface samples.

RESULTS

Cross section analysis

The earlier survey period between 2000 to 2012 has an average depositional rate of 0.00 m/yr with a standard error (±) of 0.00 m/yr (number of cross sections (n) =196) for the entire study area from rkm 3.3 to 35.2. The later survey period between 2012 to 2018 has an average incisional rate of -0.01 ± 0.02 m/yr (n=196) (Table 3). The two-tailed t-test for both survey periods show no significant net change in bed elevation (Table 3). Changes in bed elevation of the cross sections oscillate spatially along the study reach with no significant trend or pattern in incision or deposition (Fig. 8).

Even though the levee setback and landslide sub-reaches have individual cross sections with elevation changes that exceed ± 0.05 m/yr, there is not significant change in the net average elevation within the sub-reaches (Fig. 8). The levee setback at Cedar River Rapids has an average bed elevation change of -0.02 ± 0.02 m/yr within the early survey period right after construction and -0.00 ± 0.03 m/yr in the later survey period (n=4). Rainbow Bend, the second levee setback upstream, was constructed in 2014 and has a 0.02 ± 0.04 m/yr change between 2012 and 2018 (n=9). The 2001 landslide sub-reach shows an average change in bed elevation of 0.02 ± 0.02 m/yr from 2000 to 2012 and -0.04 ± 0.04 m/yr from 2012 to 2018 (n=6). The two-tailed t-test shows that the net average of channel bed elevation changes within the sub-reach is not statistically distinguishable from zero net change at a 95% confidence interval (Table 3).

Bluff grain size analysis

The images collected for the optical granulometry methodology to measure bluff grain size distributions have a varying degree of resolution, which influences the effectiveness of the

software to measure actual grains. The BASEGRAIN detection software measures a resolution range of 5.3 - 4.8 mm/px from the orthoplane images in areas A and B using the ruler and hammer as scales (Table 2). The individual drone image resolutions range from 3.0 - 4.1 mm/px, and the hand-held images have a higher resolution ranging from 0.2 - 0.1 mm/px. Both of these individual images were not orthorectified and therefore have a potentially skewed resolution from the scale at the base of the bluff to the upper sections of the bluff. Had the laser scale described in the methods section worked, the skewed resolution from the non-orthorectified images could have been adjusted for the upper and lower sections but, because there was not a scale at the upper end of the bluff, it was not possible determine if the image resolution was skewed. In this study the most accurate detection resolution compared to the grab sample sieve analysis is 4.1 mm/px taken from the individual drone image in area B (Drone B) (Fig. 10). To reduce the error in measuring grain sizes in the images, Graham's (2005) smallest detectable grain size threshold of 23 px was used to truncate the smallest grain size measured from the Drone area B image at ~95 mm or larger (Table 2).

Based on the resolutions of the images collected in the field, the measured grain sizes detected in the software outputs, and error removal using Graham's (2005) detectable grain size threshold, we assume the optical imagery grain size distributions for grain sizes 95 mm or larger are reliably measured in the bluff. Using the average of all the drone images from A and B areas (excluding the outliers in Figure 10) 18% of the bluff particles are larger than 95 mm (Fig. 10). The grab sample and percent sand lens are used to determine sediment smaller than 95 mm in the bluff. The grab sample represents the particle distribution of grains smaller than the largest sieved grain size at 90 mm. The orthoplane imagery was used to map the proportion of sand lenses, which encompassed 4.7% of the total A and B areas of the bluff (Fig. 4). The sand lenses

mapped in the bluff are assumed to be composed of 100% sand. The total sand in the bluff face (2 mm or smaller) is estimated by combining the grab sample measurements of sand and smaller grain sizes with the sand lens percent and scaling it to the 18% of 95 mm grains and larger image grain size distribution from the image analysis (Fig. 11). 21% of the bluff is estimated to be comprised of sediment 2 mm or finer based on combining the facies mapping and the grab sample. The proportion of gravel and cobbles supplied from the bluff is estimated to be 79% of the bluff distribution.

The grain size distribution from the bluff and subsurface samples collected by King County (1993) and USCOE (1994) in the Renton reach have a similar percentage of material larger than 2 mm (Fig. 12) (Table 5). The subsurface samples collected from rkm 2.5 to 0.3 have proportions of gravel ranging from 82% to 61% with an average of 73%. The estimated bluff grain size distribution has a 79% proportion greater than sand. The estimated median grain size in the bluff material, after reducing by one fourth in size due to attrition during transport to the Renton reach, is approximately 32 mm. The bed material median grain sizes fine downstream from rkm 2.5 to rkm 0.3 and have a median grain size of 27 mm and 14 mm, respectively. The proportion of gravel in the Renton reach at rkm 2 is 79%, which is the same as the estimated proportion of material coarser than 2 mm in the bluff.

DISCUSSION

Channel bed elevation changes

This study investigates bed elevation change as a potential source of sediment contributing to the aggrading channel in Renton. Bed elevation in the Cedar River from rkm 3.3 to the Landsburg Diversion shows no significant net change for the entire channel from Landsburg to rkm 3.3. Recent alterations from levee setback areas and a landslide also showed no localized net change in bed elevation. Therefore, over the last 18 years, changes in channel bed elevation upstream of Renton to Landsburg are not significantly contributing to the aggradation of the channel in Renton. The predicted channel incision following bank armoring (Perkins et al., 2002) has not altered bed elevation in the last 18 years.

Bluff sediment sizes and implications for downstream contributions

While bluffs contribute 49% of the sediment to the Cedar River (Perkins et al., 2002), it is not just the quantity of the material in the bluff contributing to the river, but it is also the size of the material that is important to understand deposition in Renton. For example, a glaciolacustrine bluff, primarily composed of clay and silt, and would not contribute to the bedload in the Renton reach, instead it would be transported in suspension to Lake Washington. The bluff characterized in this study is estimated to have a high proportion of coarse material that will contribute to the bedload in the Renton reach (Fig. 12), but does not necessarily represent all the eroding bluffs along the river. Perkins et al. (2002) estimated the bluff characterized in this study contains 95% gravel, which is 16% greater than the gravel proportions found in this study. However, other bluffs below Landsburg were estimated to have gravel proportions between 100% to 40% gravel.

This suggests that the bluff characterized in this study does not necessarily represent all the bluffs contributing sediment to the Cedar River.

The estimated 79% of the bluff grain size distribution larger than sand is similar to the bed material samples in the Renton reach, especially for samples taken between rkm 2.5 and 1 (Fig. 12). Because the grain sizes in the bluff are primarily coarse material, the bluff is a particularly important source of material to the Renton reach. However, due to attrition, the coarse material from the bluff, contributed to the river at rkm 33.4, reduces in size based on the distance transported and the hardness of the paticles (e.g. O'Conner et. al, 2014). Most of the bluff sediment sources to the Cedar River are in the upper 8 rkm below Landsburg (Perkins et al., 2002). One mill tumbling experiment for continental outwash deposits from the Olympic Mountains in Washington (Collins and Dunne, 1989) with similar lithologies and origins as the outwash glacial bluff material, suggests that even relatively hard outwash particles will reduce in size during transport. Based on the tumbling experiment results, a quarter of the coarse material in the bluff is expected to be lost over 30 rkm to attrition. With the reduction of bluff material sizes, approximately 60% of the coarse bluff material is contributing to the Renton reach. The median grain size of the assumed grain sizes of the bluff after transport over the 30 rkm to Renton are just slightly larger in size as the median bed material sizes between rkm 2.5 and 2. The proportions of sand become greater lower in the Renton reach allowing for the ~21% of the sand sized bluff particles to also contribute to the aggrading bed in Renton (Table 5). Therefore, the eroding bluff material at rkm 33.4 is an important driver for the increasing flood frequency and the need to dredge in Renton.

Optical grain size detection methodology

A major limitation to the optical grain size detection method used in this study was the difficulty in getting high resolution images to reliably detect small clasts in the bluff. The conditions in the field during image collection made it difficult to collect consistent high-resolution images of the bluff. Due to wind blowing along the bluff face, the drone could not safely fly closer than ~6-10 m from the bluff. In calmer conditions, it would be possible to take closer images and multiple images of the bluff to process a higher resolution orthoimage. Kadota et al., 2016 found a drone camera with specs two megapixels higher than the camera used in this study could detect grains >10 mm with images taken 1 to 3 meters from the analyzed surface. A drone was used because of high flows during the field visit in January. During low flows, data could be safely collected standing at the base of the bluff to capture up-close images at a consistent distance from the bluff. To capture upper sections of the bluff, a rod could be used to extend the camera as high as feasibly possible for the length of the rod. Based on the results from the hand-held photographs in this study, textures in clasts with a higher moisture content and shadows stand out more during image processing (Fig. 7). When taking close-up photographs using hand held cameras it is important to pay attention to the moisture content and shadows in the individual clasts to reduce errors in the processing and the need for extensive post-processing analysis.

The cohesive sand between clasts and the loose debris on the bluff covered distinct edges of clasts used to detect grain sizes in the imagery. Grain sizes smaller than the 23-pixel threshold from Graham's (2005) image processing procedures were detected in the bluff image analysis but, detection errors increased with less pixels. Edges of smaller grains were not detected in the post-processing correction staged of the procedure. Images of fresh, over-hanging bluff faces can reduce excess debris cover that obscures particles edges in the bluff and could improve the

detectable threshold of grain sizes. If the resolution of the imagery is higher and there is minimal sand debris obscuring the clast, the edges of the clasts could be recognized in post-processing and the grain size threshold could be reduced to detect smaller grain sizes.

The bluff distribution results from optical granulometry, and facies mapping, although improvable and requiring more post-processing analysis, gives a more objective estimate of cobbles and sand grain sizes than previous visual estimations. By averaging all analyzed image grain size distributions from subsections of upper and lower areas of the bluff, a spatially representative proportion of the large cobbles was determined for the bluff. To account for sand lenses in the bluff, the orthoplane was used to estimate a proportion of sand lens facies, which is a more objective method than previous estimates. Although the estimated 4.7% of sand lenses from facies mapping is similar to Perkins et al. (2002) previous visual estimates of 5%, this gives only a minimum estimate of sand in the bluff. The grab sample grain size distribution, although not representative of the entire bluff, reveals there is also a sand proportion of approximately 16% in areas containing coarse material in the bluff. This study shows how imagery of bluff deposits can help give a more objective minimum estimate of sand facies but is an underestimate of the total sand proportions and further analysis of sand in the coarse bluff material needs to be accounted for to get the total proportion of sand. Using higher resolution images for optical granulometry would bridge the gap between minimal sand lenses estimates and large clasts to give a more accurate distribution of bluff grain sizes contributing to the Cedar River.

CONCLUSION

This study set out to determine whether channel incision in the Cedar River is contributing sediment to the depositional zone in Renton. It determined that there has been no significant channel incision upstream of Renton in the last 18 years. The second focus tested an optical granulometry method on a known bluff sediment source to see if it was possible to get a more accurate estimate of the proportion of bluff sediment contributing to the aggrading bed in Renton. This study estimates a cumulative grain size distribution of the entire bluff using optical granulometry, a grab sample, and facies mapping of sand lenses. The grain size detection method measures grain size distributions of a large eroding bluff for cobbles or larger. While optical grain size could not detect fine grain sizes, an estimate of bluff grain size distribution is determined using grab sample and facies mapping of sand lens. As the coarse material in the bluff is transported downstream, approximately one fourth of the mass is expected to be lost to attrition before reaching Renton. From the digital grain size detection results, a grab sample, and mapping the proportion of sand lenses on the bluff, 79% of the bluff material is estimated to be coarser than sand (2mm) instead of the previously estimated 95%. Grain size detection did not give an accurate result for particles smaller than small cobbles because of the resolution of the imagery used. Therefore, the detection method failed to give an overall more accurate grain size distribution measurement than previous visual estimates. The imagery did obtain a reliable proportion of sand lens facies in the bluff. By combining the grab sample sand proportion within the coarse material, this study estimated there is more sand in the bluff than previously estimated. The estimated bluff grain size distribution has a proportion of material >2 mm similar to that of the bed material samples in the upper reach of Renton. The lower section of the Renton reach has a high proportion of sand where the bluff sand proportion could potentially be

depositing. Therefore, the eroding sediment from bluffs is an important source of material contributing to the aggradation and reduced channel capacity in the City of Renton.

REFERENCES

ASTM C136/C136M, 2014, Standard Test Method for Sieve Analysis of Fine and Coarse Aggregates, ASTM International, West Conshohocken, PA.

Booth, D.B., 1995, Geologic Map of the Maple Valley Quadrangle, King County, Washington. Miscellaneous Field Studies Map MF-2297. U.S. Geological Survey, Reston, VA.

Butler, J. B., Lane, S. N., and Chandler, J. H., 2001, Automated extraction of grain-size data from gravel surfaces using digital image processing: Journal of Hydraulic Research, v. 39, no. 4, p. 1–11.

Chrzastowski, M., 1983, Historical Changes to Lake Washington and Route of the Lake Washington Ship Canal, King County, Washington. Water Resources Investigation Open-File Report 81–1182. U.S. Geological Survey, Reston, VA.

Collins., B. D., and Dunne, T., 1989, Gravel transport, grave harvesting, and channel-bed degradation in rivers draining the southern Olympic Mountains, Washington, U.S.A.: Environmental Geology, v. 13, p. 213–214.

Collins, B.D., Montgomery, D.R., 2011, The legacy of Pleistocene glaciation and the organization of lowland alluvial process domains in the Puget Sound region. Geomorphology 126, p. 174–185.

Detert, M., and Weitbrecht, V., 2013, User guide to gravelometric image analysis by BASEGRAIN. Advances in science and research, S. Fukuoka, H. Nakagawa, T. Sumi, and H. Zhang, eds., Taylor & Francis, London, p. 1789–1795.

Eastwick, P. G., 1891, Report on survey with estimates for proposed Lake Washington Ship Canal: Portland,U.S. Engineer Office, unpublished report, p. 42.

Fehr, R., 1987, A method for sampling very coarse sediments in order to reduce scale effects in movable bed models, in Proceedings of IAHR Symposium on Scale Effects in Modelling Sediment Transport Phenomena, Toronto, Canada. p. 383–397.

Federal Emergency Management Agency., 2005, Flood Insurance Study, King County Washington and Incorporated Areas. Washington D.C.

Gendaszek, A.S., Magirl, C.S., Czuba, C.R., 2012, Geomorphic response to flow regulation and channel and floodplain alteration in the gravel-bedded Cedar River, Washington, USA. Geomorphology v. 179, p. 258–268.

Graham, D.J., Rice, S.P., Reid, I., 2005, A transferable method for the automated grain sizing of river gravels, *Water Resources Research*, 41 (W07020).

Highland. L. M., 2002, An Account of Preliminary Landslide Damage and Losses Resulting from the February 28, 2001, Nisqually, Washington, Earthquake. U.S. Geological Survey. Open file rep. 03–211

Inter-Fluve, Inc., 2000, Preliminary Assessment of Sediment Trapping Potential of Cedar River Landsburg Diversion. Prepared for Seattle Public Utilities and Duke Engineering & Services by Inter-Fluve, Inc., Hood River, Oregon.

Kadota, A., Asayama C,. Ndwambi, I, D., 2016, Image analysis of grain size distribution around area of sand deposition. River Flow 2016 Conference.

King County., 1993, Cedar River Current and Future Conditions Report. Prepared by King County Department of Public Works, Surface Water Management Division, King County, Washington.

King County., 2015, Cedar River channel migration study. Prepared by Terry Butler and Fred Lott. King County Department of Natural Resources and Parks, Water and Land Resources Division. Seattle, Washington.

McEwan, I. K., Sheen, T. M., Cunningham, G. J., and Allen, A. R., 2000, Estimating the size composition of sediment surfaces through image analysis: Proceedings of the Institution of Civil Engineers, Water and Maritime Engineering, v. 142, no. 4, p. 189–195.

Mullineaux, D. R., 1970, Geology of the Renton, Auburn, and Black Diamond quadrangles,

King County, Washington. Professional Paper. U.S. Geological Survey, 672. Washington, D.C.

Northwest Hydraulic Consultants Inc., 1995, Cedar River Sediment Data Collection and Analysis 1994 –1995.

Northwest Hydraulic Consultants Inc., 2001, Data collection for the Cedar River Report.

Northwest Hydraulic Consultants Inc., 2017, Cedar River 2017 Annual Sediment Report.

Perkins Geosciences and Harper Houf Righellis, Inc., 2002, Cedar River gravel study phase 2 report. Unpublished report to U.S. Army Corps of Engineers, Seattle District Office and Jones & Stokes, Bellevue Washington. p. 67

Prych, E.A., 1988, Flood-conveyance capacities and changes in channels of the lower Puyallup, White, and Carbon Rivers in western Washington: U.S. Geological Survey Water-Resources Investigations Report 87-4129, 43.

Sime, L. C., and Ferguson, R. I., 2003, Information on grain sizes in gravel-bed rivers by automated image analysis: Journal of Sedimentary Research, v. 73, no. 4, p. 630–636.

Timm R.K., Wissmar R.C., 2013, Response to disturbance in a highly managed alluvial river: does it conform to Le Chatelier's general law? *Geomorphology* 182: pp.116–124.

USCOE., 1997, Final Detailed Project Report Cedar River Section 205 Renton, Washington, US Army Corps of Engineers, Seattle District.

FIGURES

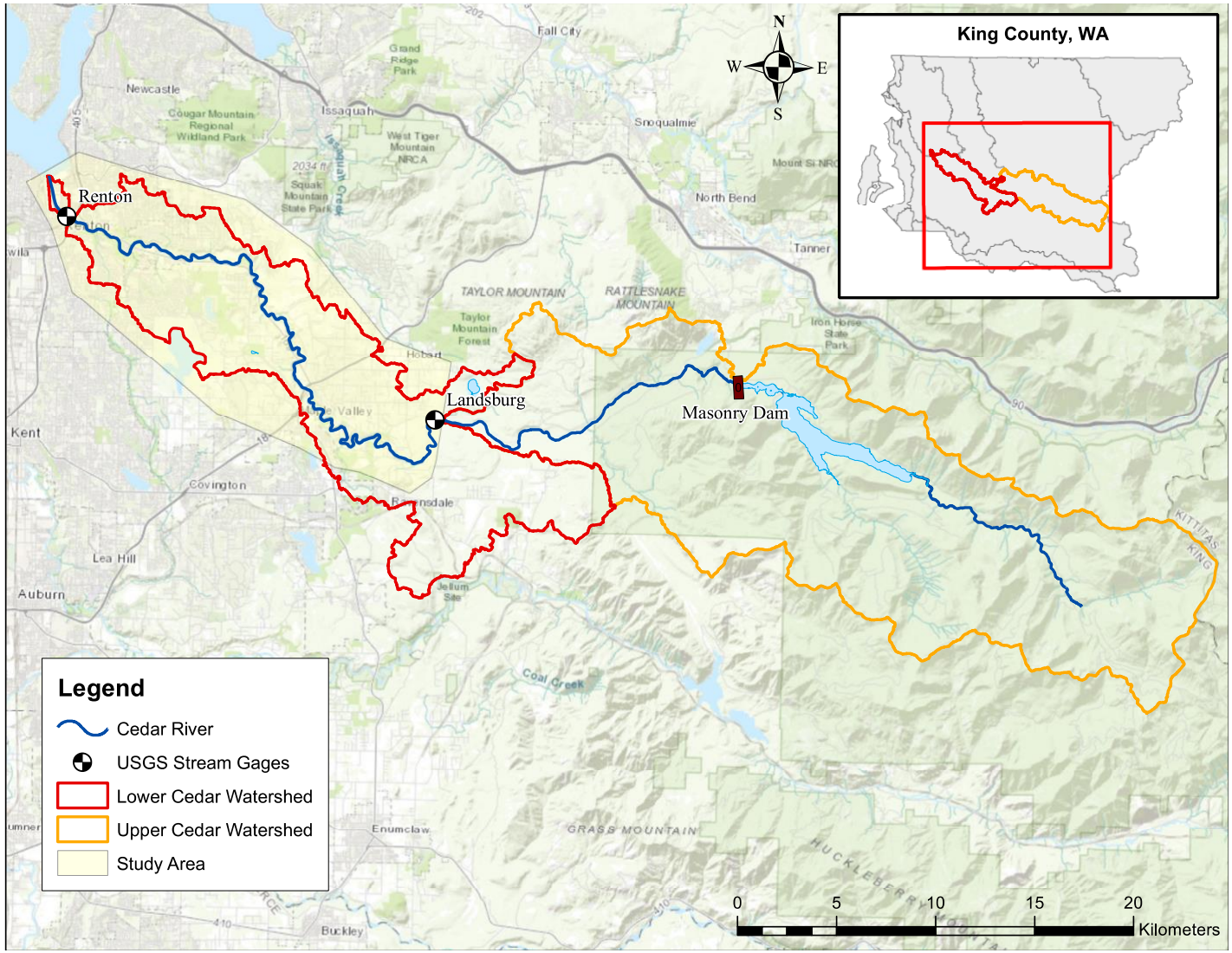

Figure 1. Site Map of the Cedar River Watershed, King County Washington.

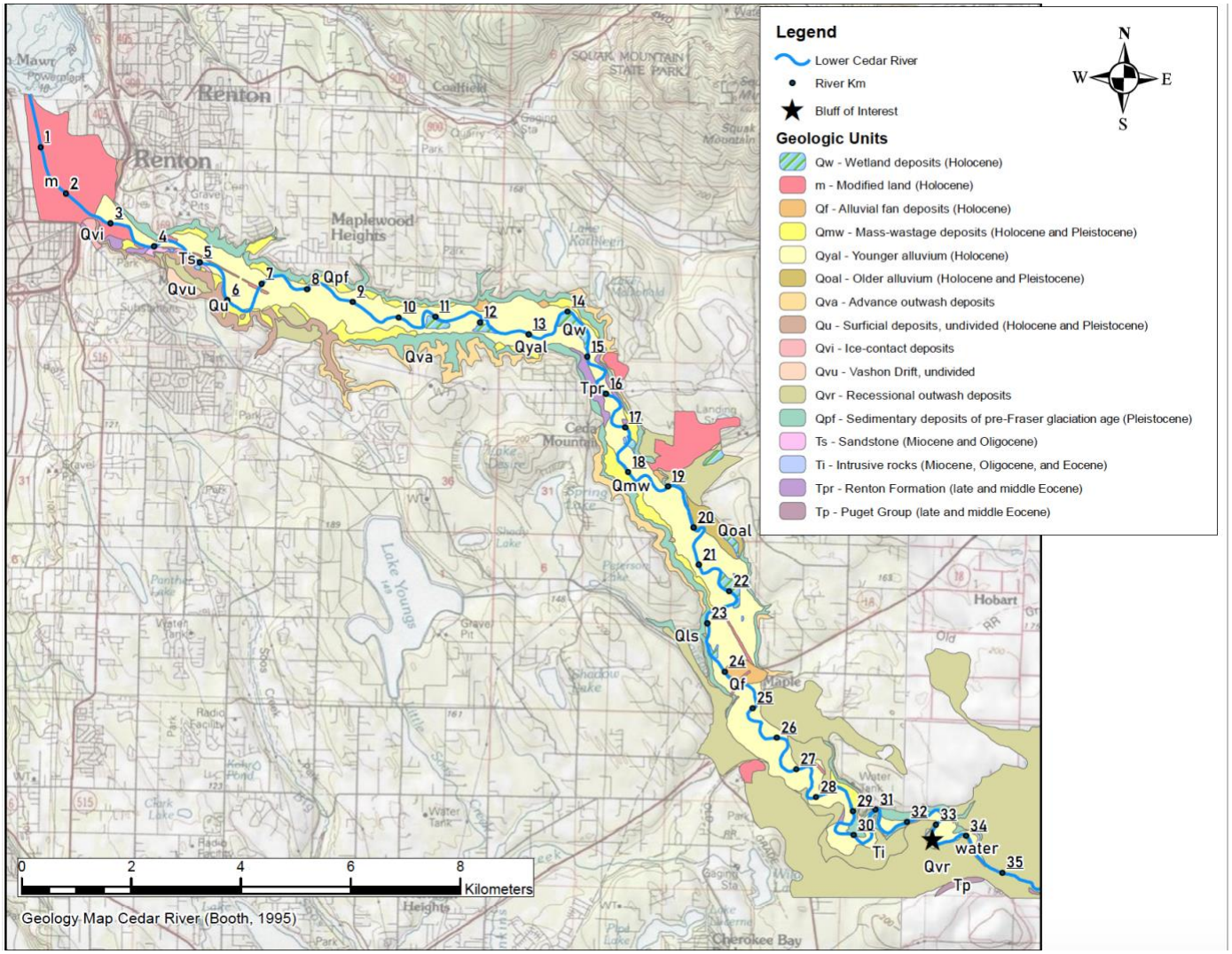

Figure 2. Geological map of study area (Booth, 1995). Eroding glacial outwash bluffs are predominantly located between rkm 36 and 29. The bluff characterized in this study in located at rkm 35. 5 within the recessional outwash deposit (black star).

Figure 3. Eroding bluff of interest at rkm 33.4 characterized for cumulative grainsize distributions using image analysis. Maximum bluff height is 33.4 m. Photo is taken from the right bank. River is flowing from left to right.

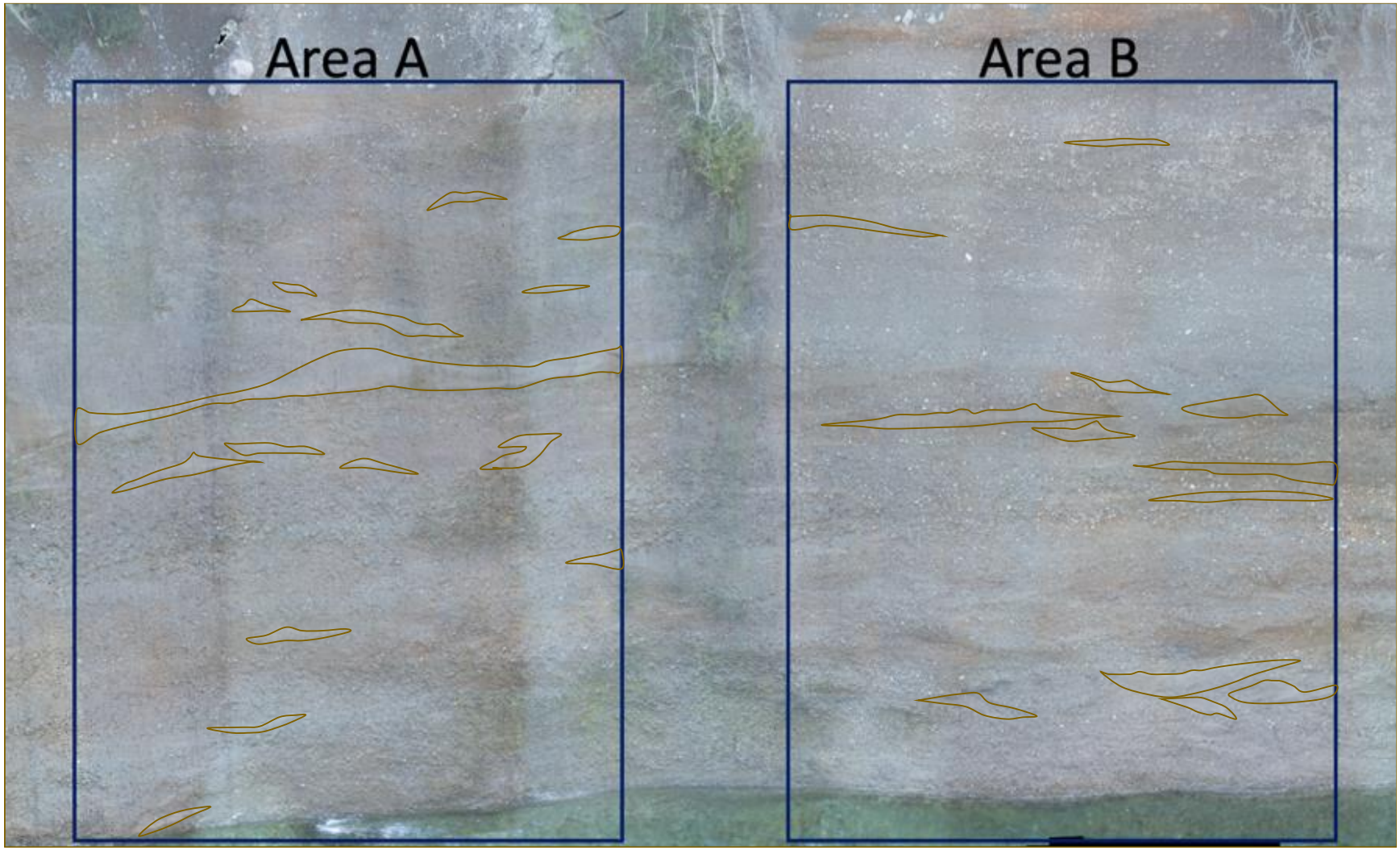

Figure 4. Facies map of sand lenses (outlined in brown) in the two sections that were analyzed for grain sized distributions.

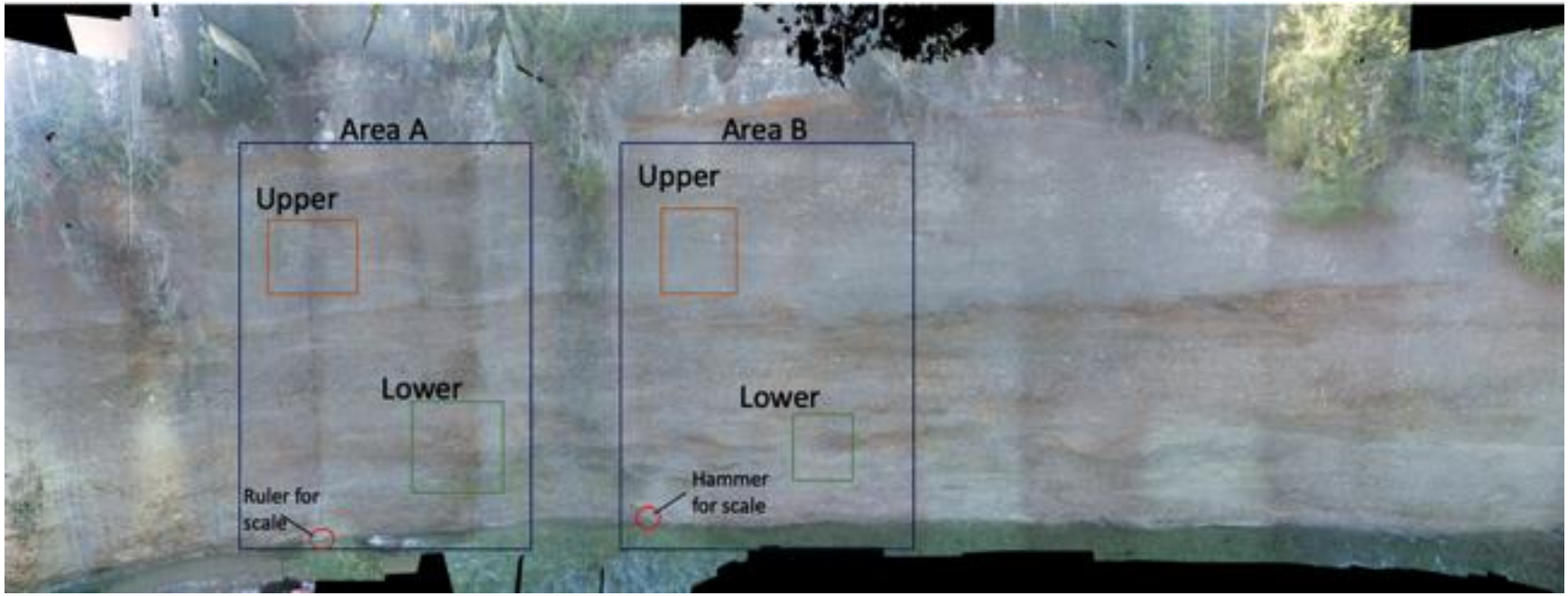

Figure 5. Orthoplane image of the bluff of interest. Ten by thirty meters section of the bluff were used for the grain size image analysis method (Area A and Area B). The scales used to determine the resolution of the processed images are marked by the red circles.

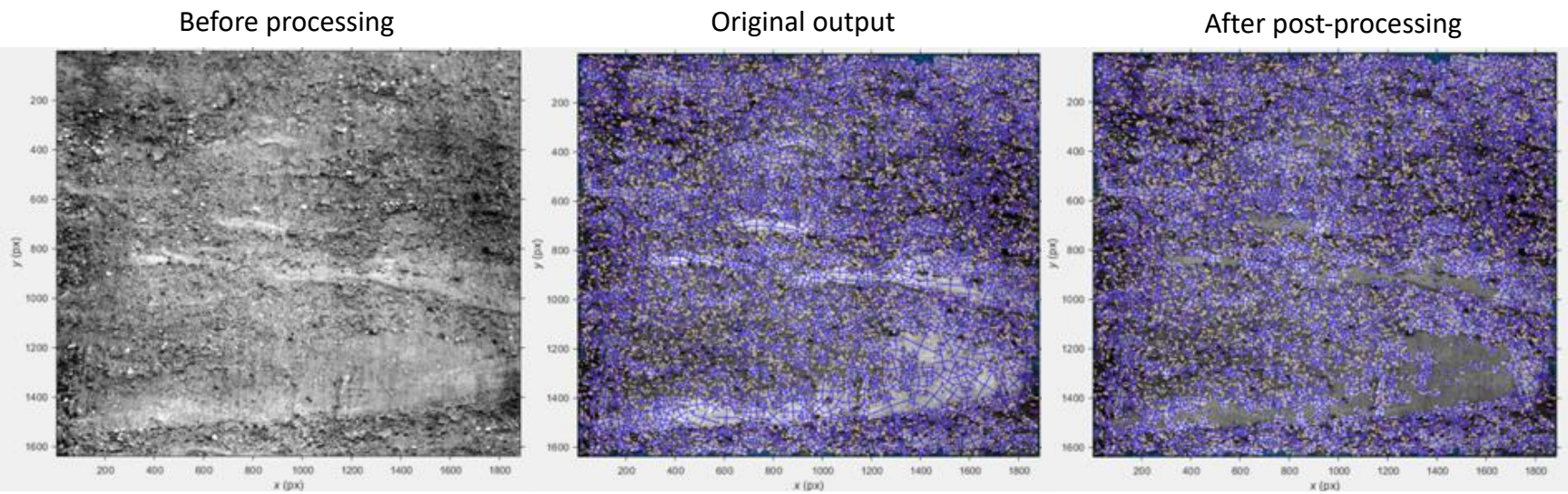

Figure 6. The image on the left shows in grayscale mode with a resolution of 5.3 mm/px ready to be processed in BASEGRAIN. The image includes several sand senses. The center image shows the original output. Sand lens detection error occurred by measuring large patches of the sand lens as individual grains. The image on the right shows the output after post-processing was used to remove the large sand lens errors.

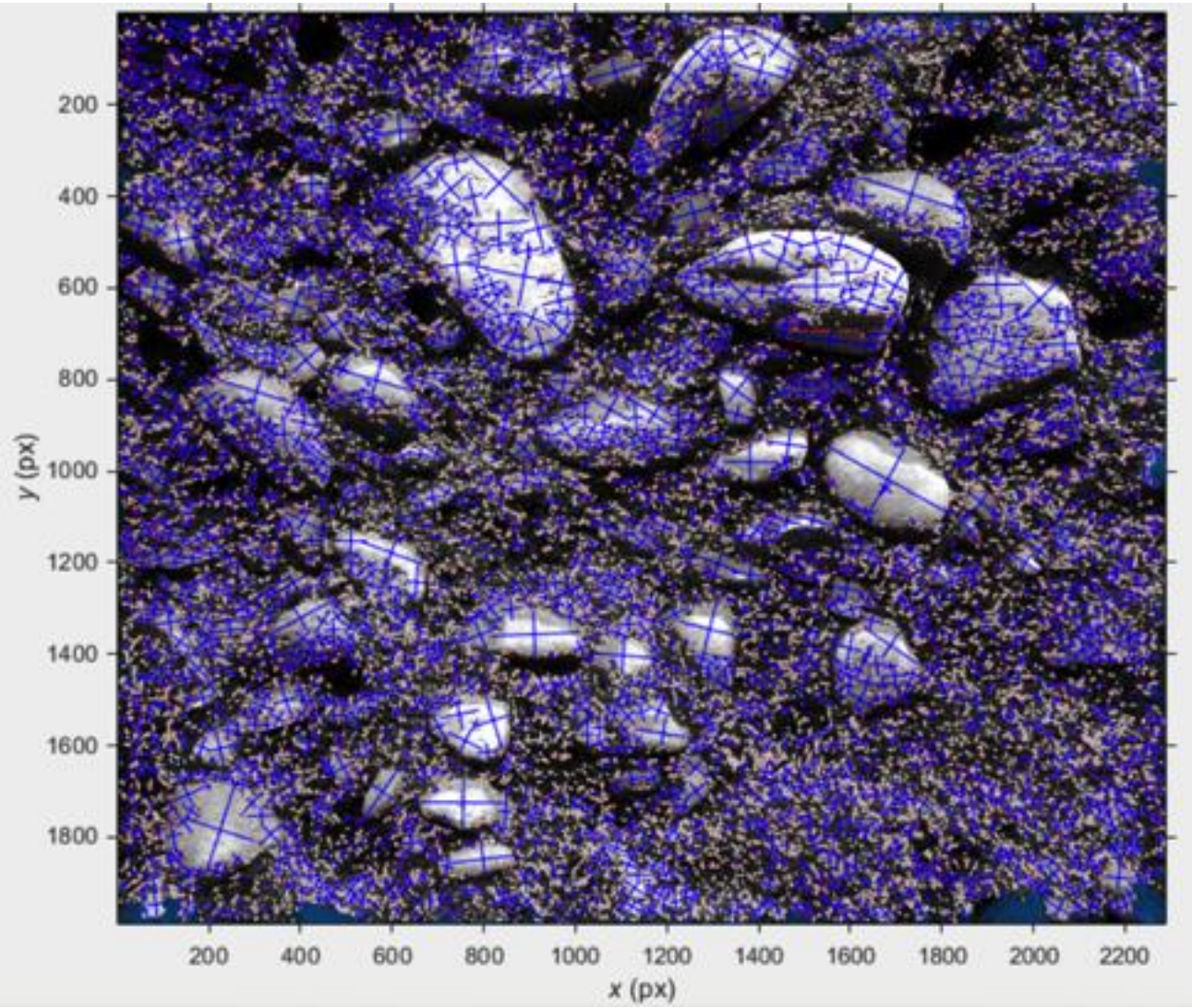

Figure 7. Image showing the initial output in BASEGRAIN of a high-resolution (0.2756 mm/px) hand-held images. The blue crosses represent the a and b axes of individual grains detected from the software. This output gives an underestimate of the actual grain sizes in this image.

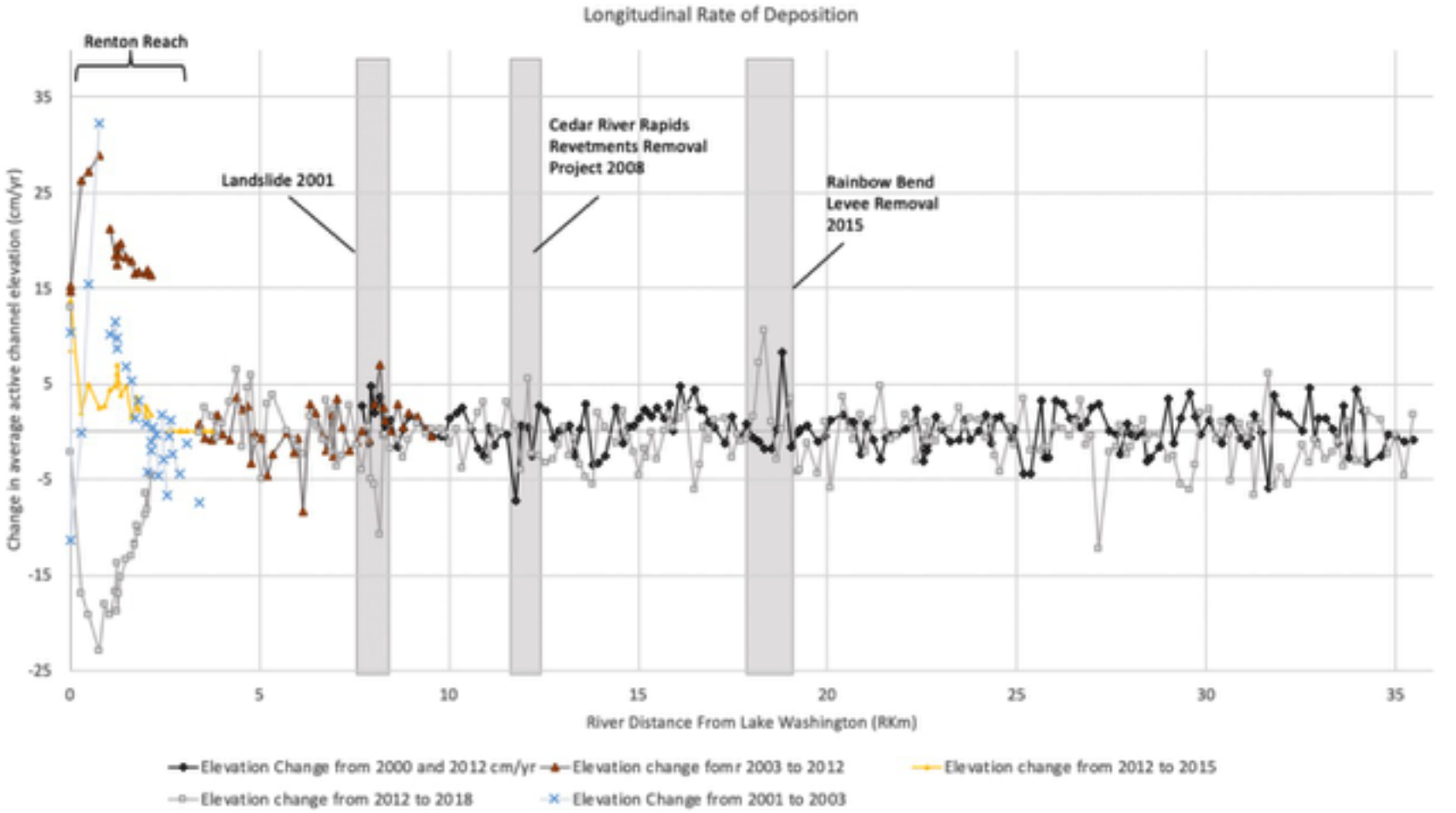

Figure 8. Rates of deposition for each cross section between 2000 and 2003 to 2012 (black line and orange triangles) and 2012 to 2018 (Gray line) along the Cedar River up to river kilometer 35.2. Landslide and Levee Setback projects sub reached are highlighted.

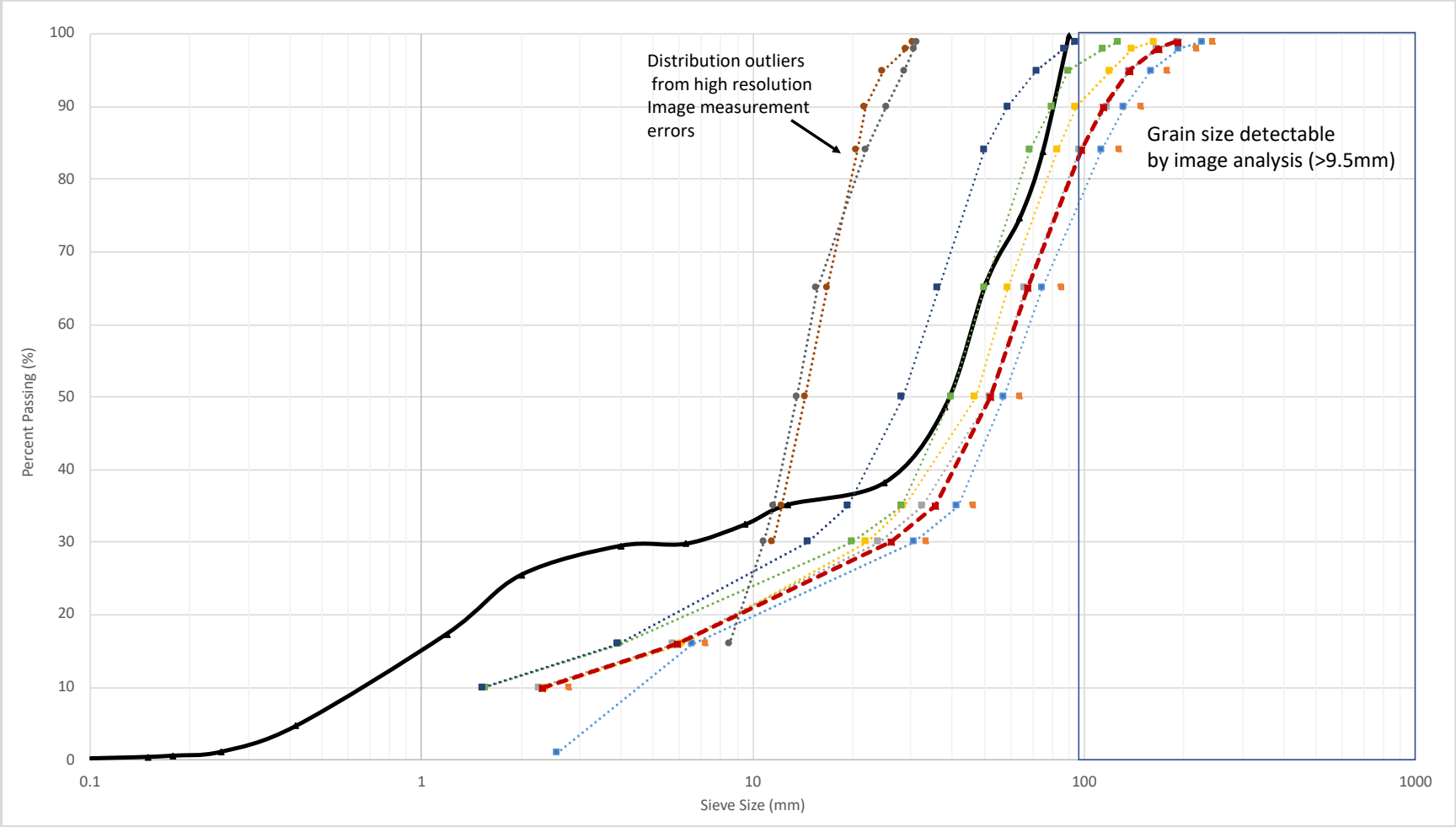

Figure 9. Grain size distribution curves for all images processed in BASEGRAIN (dotted lines) compared to the grain size distribution curve of the grab sample collected from the bluff (black line). Distributions for analyzed image distributions were averaged (red dashed line). The two high resolution hand-held camera distribution outliers (dotted line) were not used to represent the average distributions of the grain size image analysis.

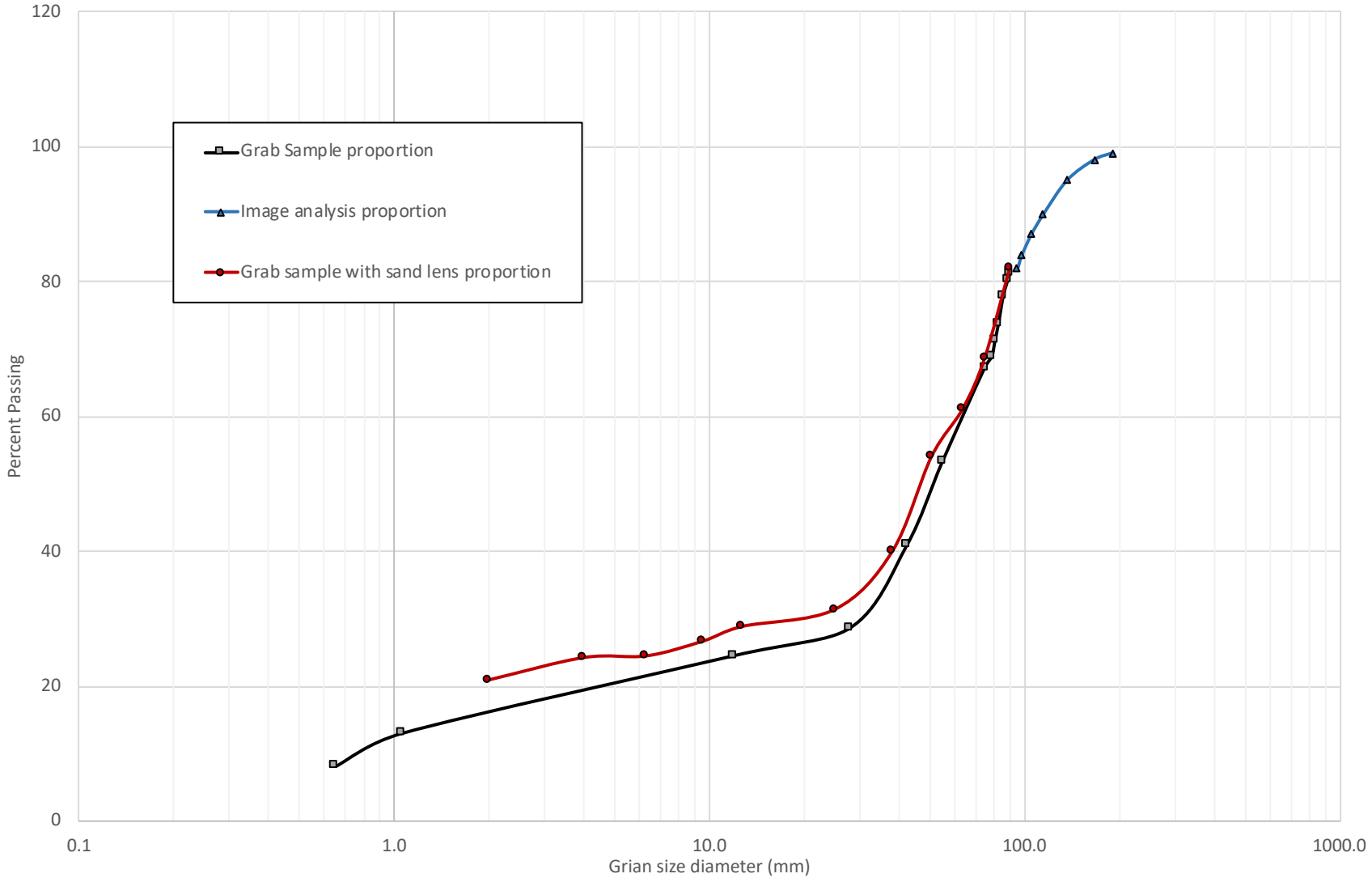

Figure 10. Estimated grain size distribution used to represent the spatial variability of the bluff at rkm 33.4. Proportions are based on image analysis grain sizes (>95mm) (blue triangles), grab sample distribution (black squares), and percent sand lenses in the bluff face (red circles).

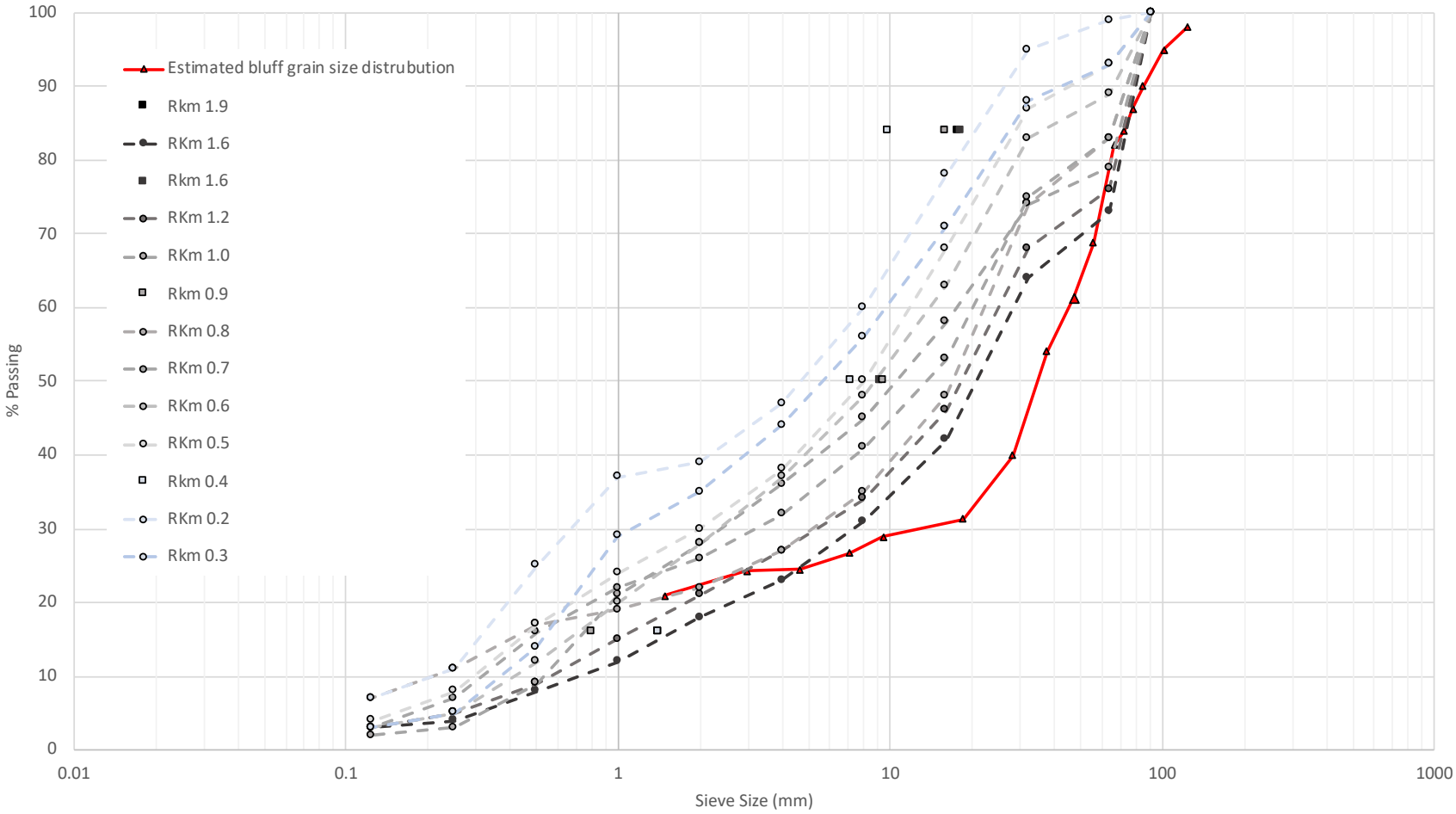

Figure 11. Comparison of the estimated bluff grain sizes distribution in Renton with bedload and subsurface samples. King County (1993) collected four substrate samples in point and lateral bars in the Renton Reach (Squares). USCOE (1994) collected 9 samples from rkm 1.59 to 0.4 of bed material using McNeil samplers (dashed lines with circles). The estimated bluff grain size distribution after reducing 26% in size during transport to Renton (red line with triangles) has similar or coarser grain sizes than the bed material in Renton.

TABLES

Table 1. Levee setback projects along the Cedar River and a measured maximum width of floodplain/channel that was opened to the channel.

Name	Date completed	Upstream extent (rkm)	Downstream extent (rkm)	Bank	Change in channel/floodplain width (m)
Cedar River Gravel Removal	1998 & 2016	2	0	Channel bed	N/A
Cedar River Rapids	2012	11.9	11.5	Right	+122
Rainbow Bend	2014	17.21	18.51	Right	+14

Table 2. List of images from subsections on the bluff analyzed in the object detection software, BASEGRAIN. The resolution of the images was measured by the scales included in the images. Smallest grain size detected is based on the limit of 23 pixels needed to detect an object and the mm/px resolution. The analyzed images size represents the processed area for grain sized distributions for each section.

Images	Resolution (mm/px)	Graham's (2005) truncation threshold approximate smallest Grain detected (mm)	Analyzed area (m^2)
Lower A	5.3	122	130
Upper A	5.3	122	83
Lower B	4.8	111	50
Upper B	4.8	111	100
Drone A	3.1	71	18
Drone B	4.1	95	14
Ruler 1	0.2	5	0.1

Table 3. Table shows sections of bed elevation change averaged along the Cedar River. Standard errors and t-test values are displayed. Resulting net deposition or no net change are determined using a 95% confidence interval with the t-value.

Reach and Sub-reach locations			**Early Survey Period (between 2000 to 2012)**				**Later Survey Period (between 2012 to 2018)**			
Reach Name	Downstream extent (Rkm)	Upstream extent (Rkm)	Average Rate of Deposition from 2000 to 2012 (m/yr)	Sample size	t-value	Significant Change	Average Rate of Deposition from 2012 to 2018 (m/yr)	Sample size	t-value	Significant Change
Renton depositional zone	0	3.3	0.18 ± 0.02	23	21.15	Net Depositon	-0.12 ± 0.02	22	-7.38	Net Depositon
Entire Study Area (From Top depositional zone to Landsburg Dam)	3.3	35.2	0.00 ± 0.02	196	1.23	No Net Change	-0.01 ± 0.02	196	-0.22	No Net Change
Landslide Zone	7.7	8.3	0.02 ± 0.02	6	2.12	No Net Change	-0.04 ± 0.04	6	-1.05	No Net Change
Cedar River Rapids	11.4	11.9	-0.02 ± 0.02	4	-0.93	No Net Change	-0.01 ± 0.03	4	-0.04	No Net Change
Rainbow Bend	17.2	18.5	-0.01 ± 0.00	9	-1.41	No Net Change	0.02 ± 0.04	9	0.44	No Net Change

Table 4. Grain size distributions of the grab sample and all the images processed from the bluff. The shaded columns are images that were determined to not give accurate grain size measurements of the bluff.

Distrubution (%)	Grab Sample (mm)	Lower A (mm)	Upper A (mm)	Lower B (mm)	Upper B (mm)	Drone A (mm)	Drone B (mm)	Tape (mm)	Ruler (mm)	Average (mm)	Standard Deviation
10	0.7	2.6	2.8	2.3	2.4	1.5	1.6			2.3	0.5
16	1.1	6.6	7.2	5.8	6.1	3.9	4.0	8.5		5.9	1.2
30	12.0	30.7	33.4	24.1	22.0	14.7	19.9	10.8	11.5	26.0	5.8
35	28.0	41.5	46.3	32.5	28.6	19.3	28.1	11.6	12.2	35.4	8.1
50	42.5	57.2	64.3	51.9	47.0	28.3	39.7	13.6	14.4	52.0	9.4
65	55.0	74.9	85.8	66.3	58.8	36.3	50.1	15.6	16.8	67.2	13.9
84	79.0	112.7	128.8	96.8	83.2	50.0	68.6	21.9	20.7	98.0	23.7
90	83.0	132.4	149.5	117.6	94.4	58.9	80.0	25.3	21.9	114.8	28.1
95	86.0	159.0	178.5	136.5	120.4	71.9	89.6	28.7	24.7	136.8	34.4
98	89.0	194.1	219.9	166.1	139.8	87.1	114.7	30.7	29.1	166.9	41.8
99	90.0	226.9	246.9	191.4	162.4	94.5	127.3	31.3	30.5	191.0	48.2

Table 5. Grain size parameters from the estimated bluff grain sizes, the estimated sizes after one fourth of the bluff particle mass is lost to attrition over 30 river kilometers, and existing sub-surface sediment samples from Renton.

Bluff Grain Sizes	**Sources**	**Locations**	D84 (mm)	D50 (mm)	D16 (mm)	% Sand	% Gravel
		At Bluff	79	42	1	21	79
		After 30 rkm transport	63	32	1	21	59
Sub-surface samples in Renton	USCOE (1994)	rkm 2.5	75	27	2	18	82
	USCOE (1994)	rkm 2	71	22	1	21	79
	King Co (1993)	rkm 1.9	18	9	1		
	King Co (1993)	rkm 1.6	18	9	1		
	USCOE (1994)	rkm 1.5	68	16	1	28	72
	USCOE (1994)	rkm 1.3	65	19	0	22	78
	USCOE (1994)	rkm 1.1	65	22	1	26	74
	USCOE (1994)	rkm 0.9	16	9	1	28	72
	USCOE (1994)	rkm 0.8	31	8	1	30	70
	USCOE (1994)	rkm 0.5	31	22	0	35	65
	King Co (1993)	rkm 0.4	10	7	1		
	USCOE (1994)	rkm 0.3	22	14	0	39	61

APPENDIX A. Cross sections and River Kilometer Study Area

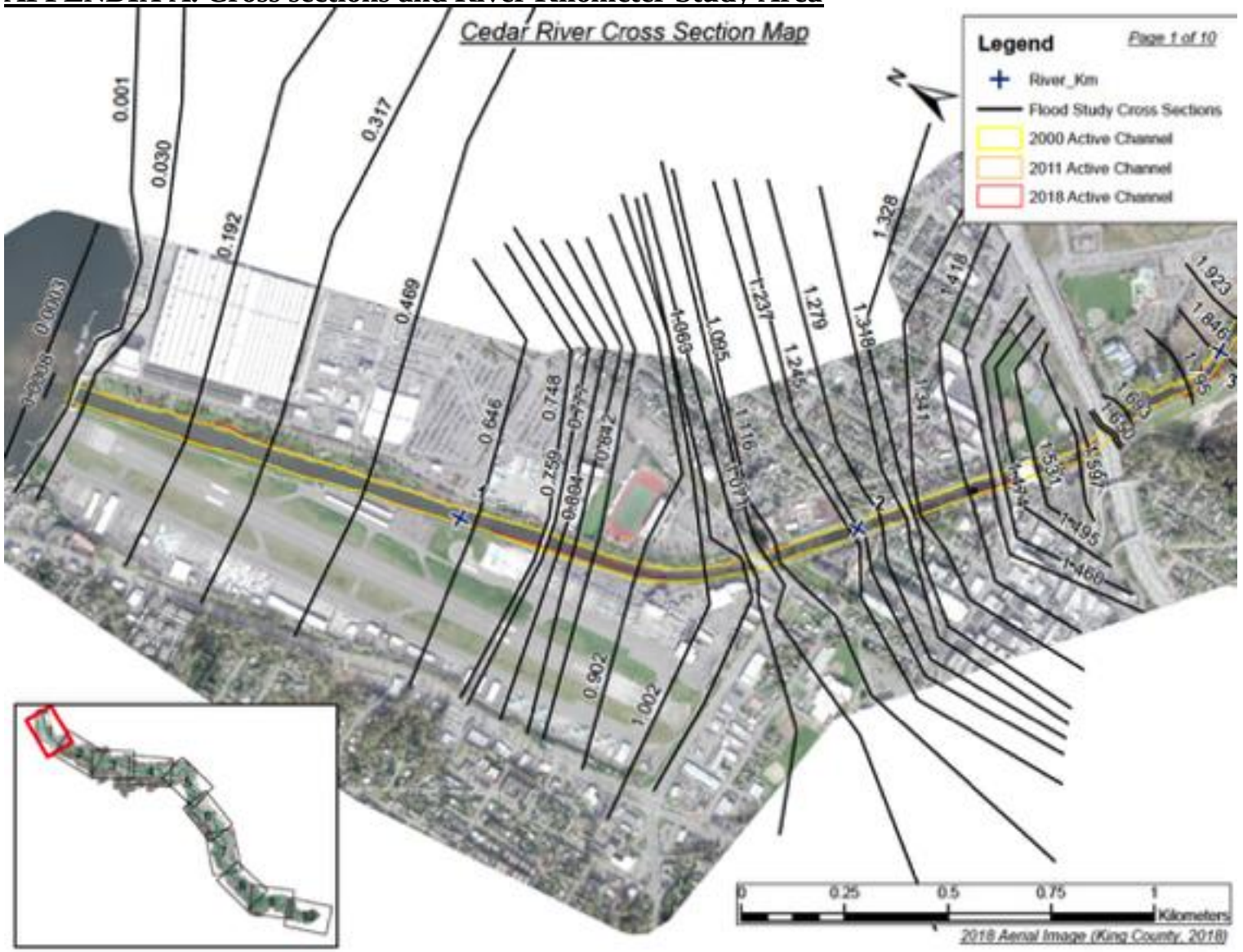

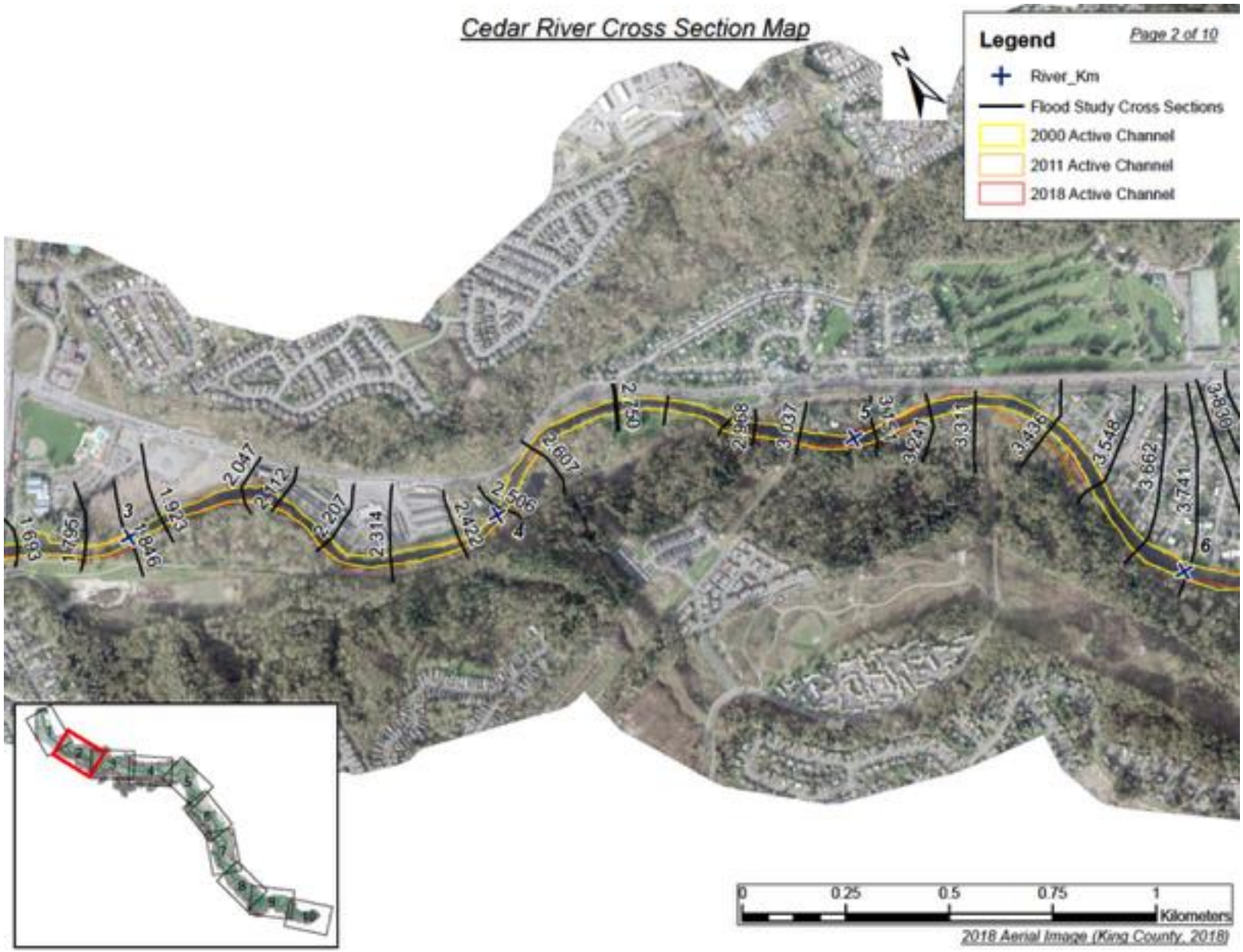
Cedar River Cross Section Map
Page 2 of 10
Legend
River_Km
Flood Study Cross Sections
2000 Active Channel
2011 Active Channel
2018 Active Channel
N
1.693
1.795
1.846
1.923
2.047
2.112
2.207
2.314
2.422
2.506
2.607
2.710
2.968
3.037
3.131
3.241
3.311
3.436
3.548
3.662
3.741
3.836
0
0.25
0.5
0.75
1
Kilometers
2018 Aerial Image (King County, 2018)

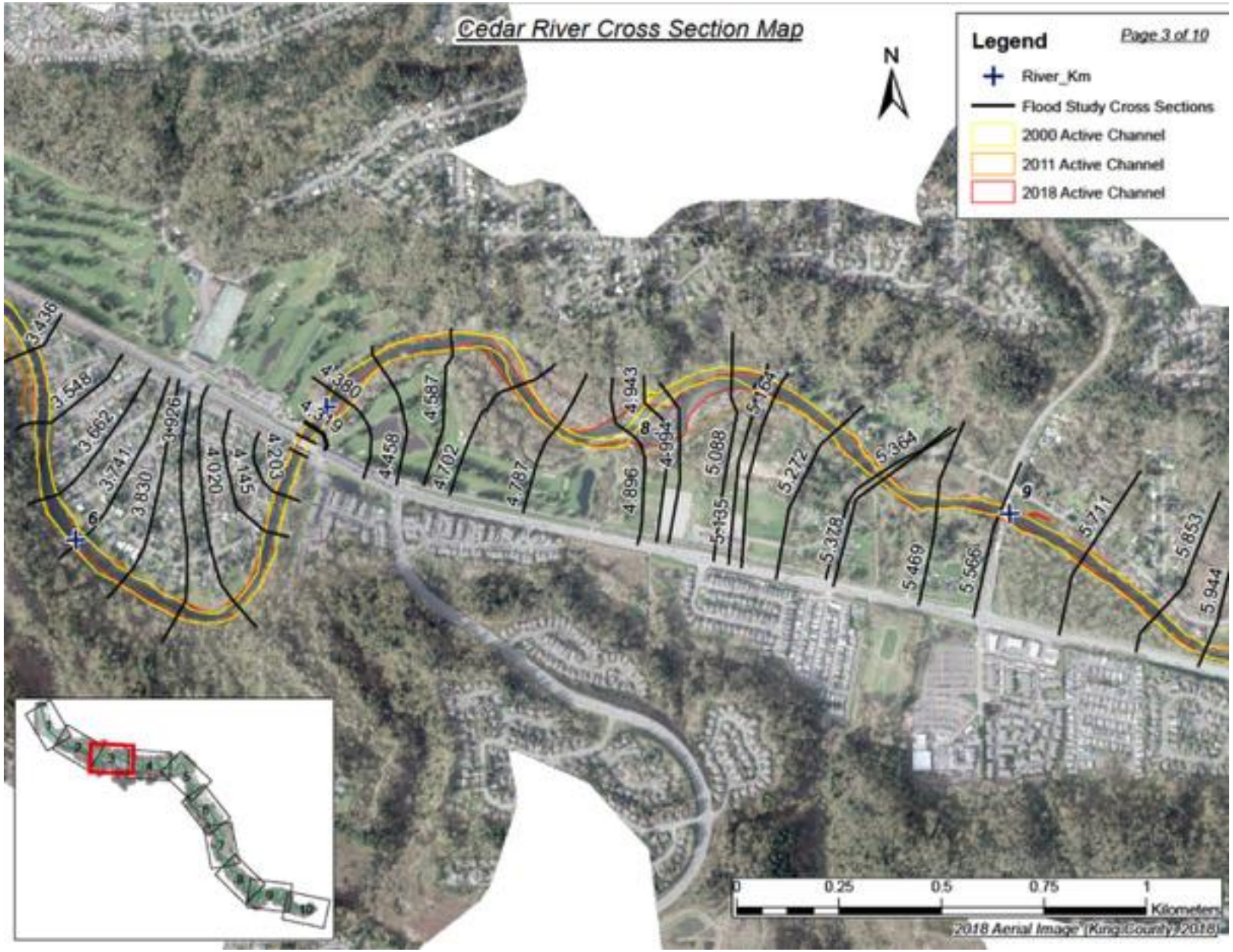
Cedar River Cross Section Map
Page 3 of 10
N
Legend
River_Km
Flood Study Cross Sections
2000 Active Channel
2011 Active Channel
2018 Active Channel
3.436
3.548
3.662
3.741
3.830
3.926
4.020
4.145
4.203
4.319
4.380
4.458
4.587
4.702
4.787
4.896
4.943
4.994
5.088
5.135
5.184
5.272
5.364
5.378
5.469
5.566
5.711
5.853
5.944
0 0.25 0.5 0.75 1
Kilometers
2018 Aerial Image (King County 2018)

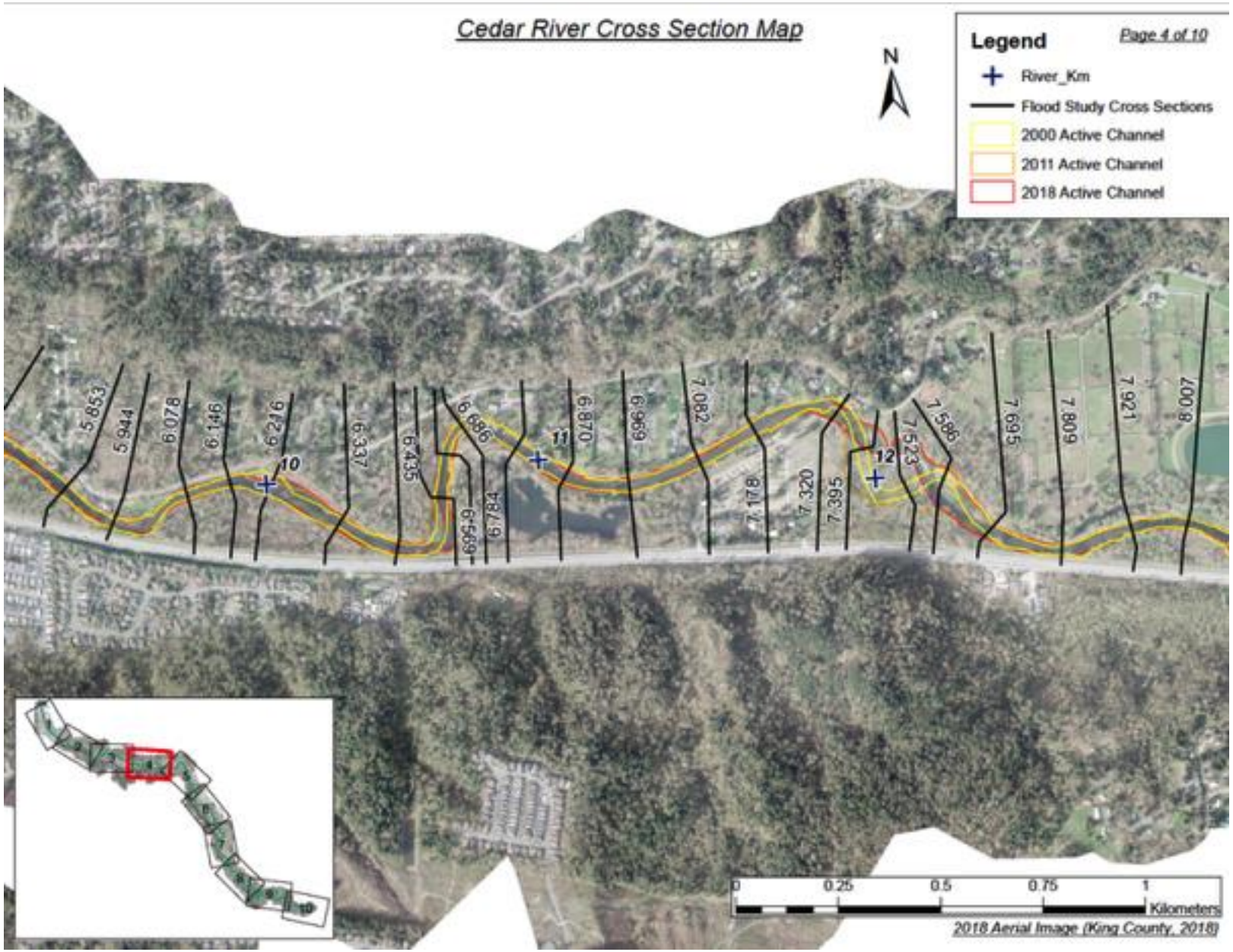
Cedar River Cross Section Map
Page 4 of 10
N
Legend
River_Km
Flood Study Cross Sections
2000 Active Channel
2011 Active Channel
2018 Active Channel
5.853
5.944
6.078
6.146
6.216
10
6.337
6.435
6.569
6.686
6.784
11
6.870
6.969
7.082
7.178
7.320
7.395
12
7.523
7.586
7.695
7.809
7.921
8.007
0
0.25
0.5
0.75
1
Kilometers
2018 Aerial Image (King County, 2018)

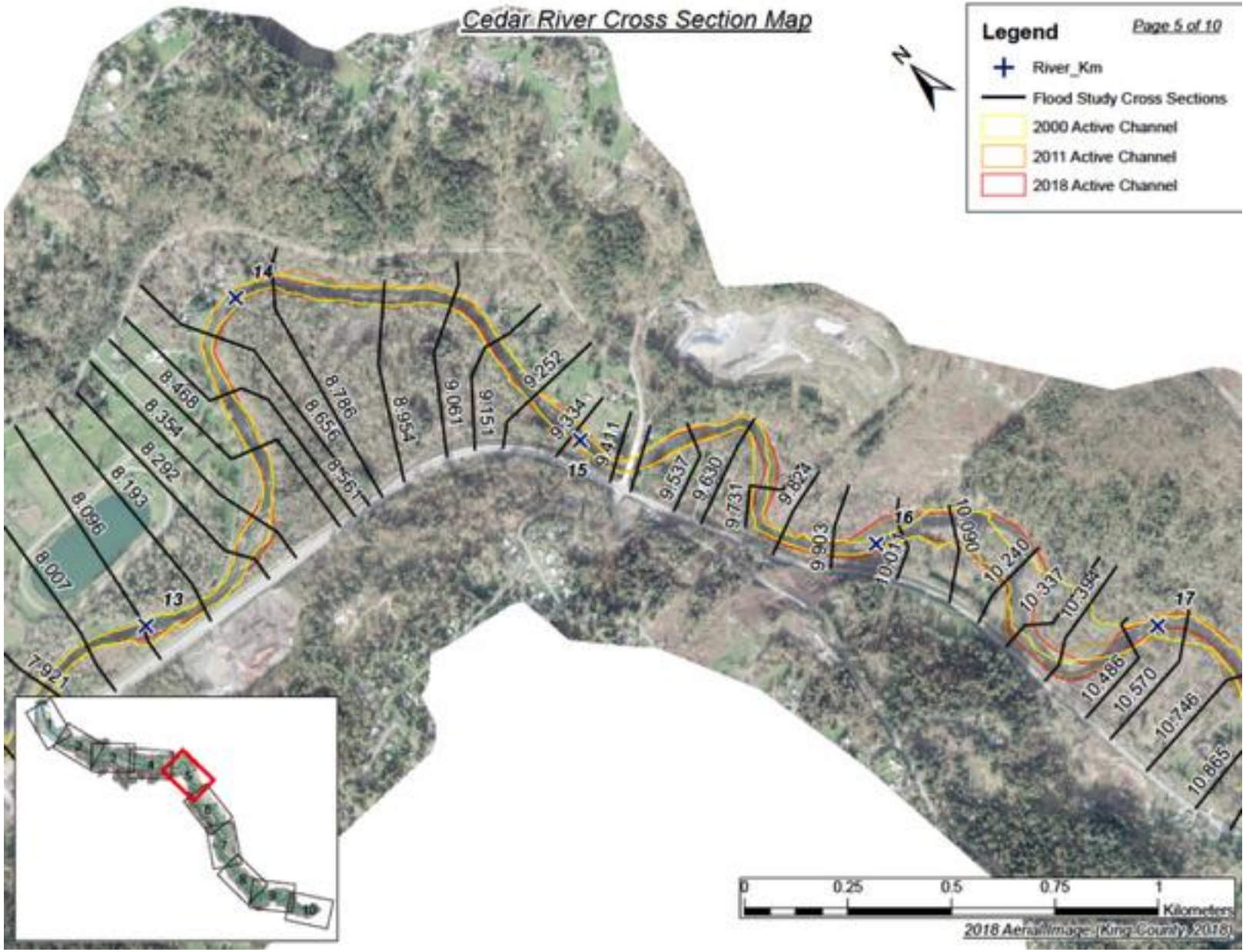
Cedar River Cross Section Map
Page 5 of 10
Legend
River_Km
Flood Study Cross Sections
2000 Active Channel
2011 Active Channel
2018 Active Channel
N
14
15
16
17
13
8.468
8.354
8.292
8.193
8.096
8.007
7.921
8.786
8.656
8.561
8.954
9.061
9.151
9.252
9.334
9.411
9.537
9.630
9.731
9.824
9.903
10.011
10.090
10.240
10.337
10.395
10.486
10.570
10.746
10.865
0
0.25
0.5
0.75
1
Kilometers
2018 Aerial Image (King County 2018)

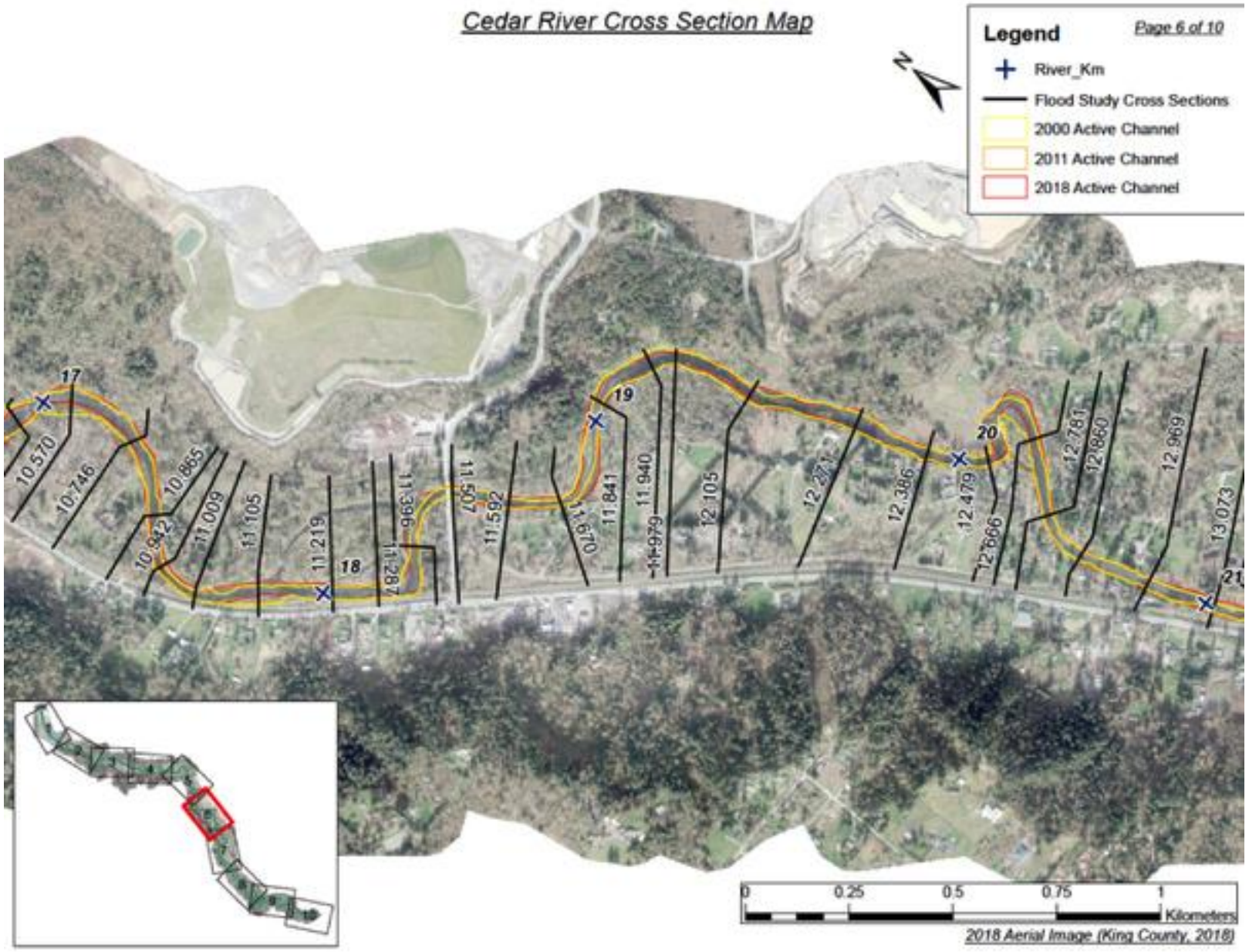
Cedar River Cross Section Map
Page 6 of 10
Legend
River_Km
Flood Study Cross Sections
2000 Active Channel
2011 Active Channel
2018 Active Channel
N
17
18
19
20
10.570
10.746
10.865
10.942
11.009
11.105
11.219
11.396
11.507
11.592
11.670
11.841
11.940
11.979
12.105
12.271
12.386
12.479
12.666
12.781
12.860
12.969
13.073
0
0.25
0.5
0.75
1
Kilometers
2018 Aerial Image (King County, 2018)

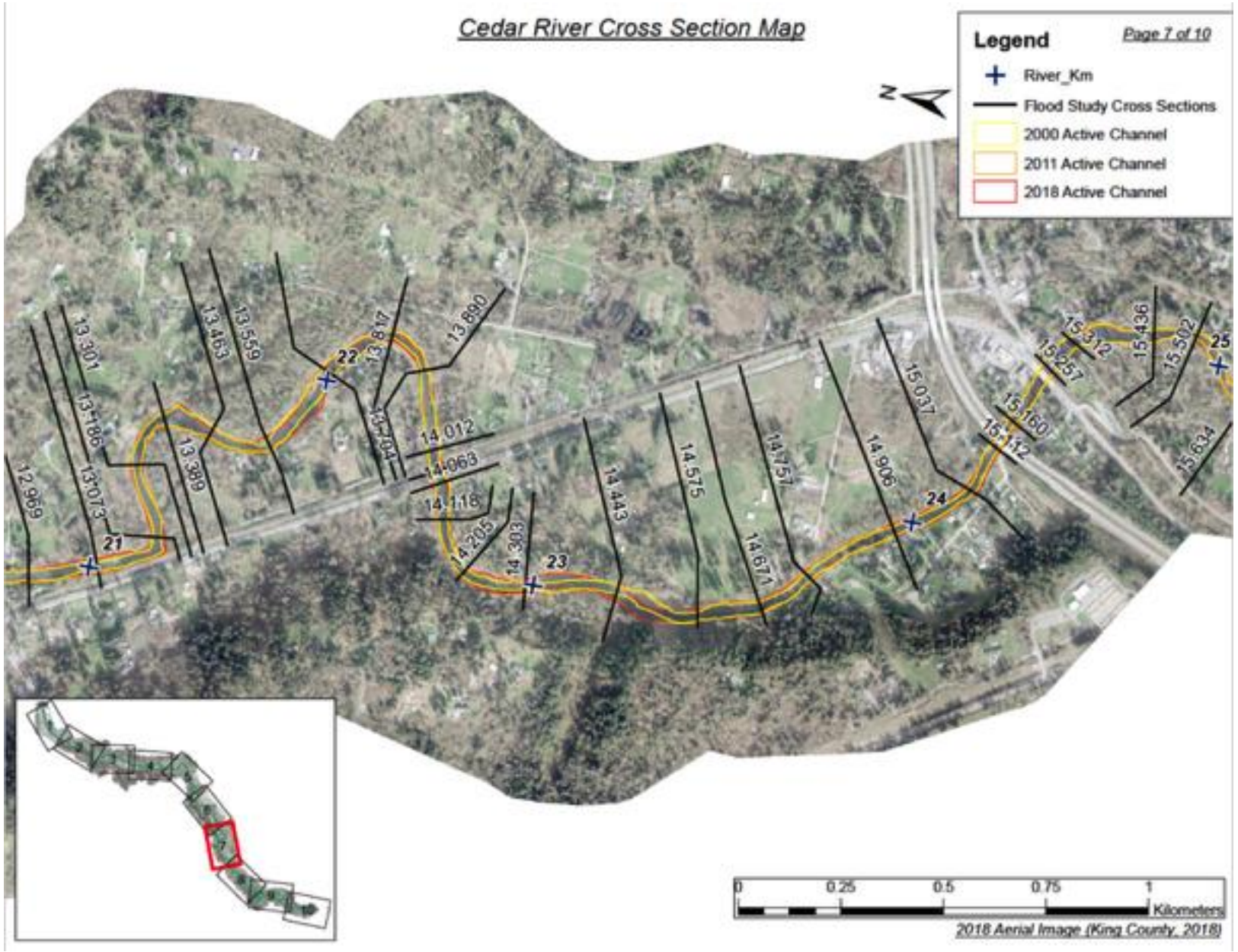
Cedar River Cross Section Map
Page 7 of 10
Legend
River_Km
Flood Study Cross Sections
2000 Active Channel
2011 Active Channel
2018 Active Channel
N
12.969
13.073
13.186
13.301
13.389
13.463
13.559
13.704
13.817
13.890
14.012
14.063
14.118
14.205
14.303
14.443
14.575
14.671
14.757
14.906
15.037
15.112
15.160
15.251
15.312
15.436
15.502
15.634
21
22
23
24
25
0
0.25
0.5
0.75
1
Kilometers
2018 Aerial Image (King County, 2018)

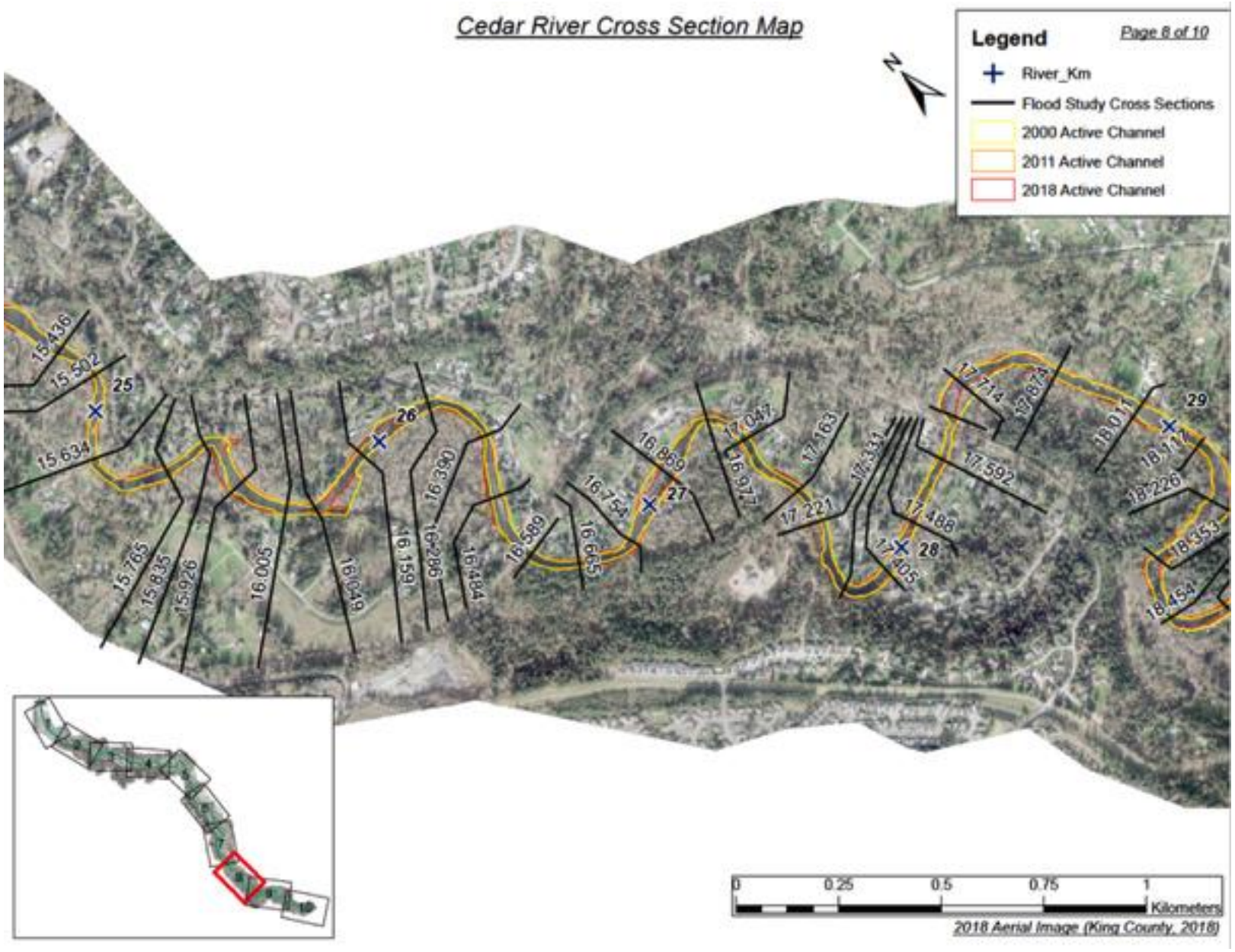
Cedar River Cross Section Map
Page 8 of 10
Legend
River_Km
Flood Study Cross Sections
2000 Active Channel
2011 Active Channel
2018 Active Channel
N
25
26
27
28
29
15.436
15.502
15.634
15.765
15.835
15.926
16.005
16.049
16.159
16.286
16.390
16.484
16.589
16.665
16.754
16.869
16.977
17.047
17.163
17.221
17.331
17.405
17.488
17.592
17.714
17.874
18.011
18.114
18.226
18.353
18.454
0
0.25
0.5
0.75
1
Kilometers
2018 Aerial Image (King County, 2018)

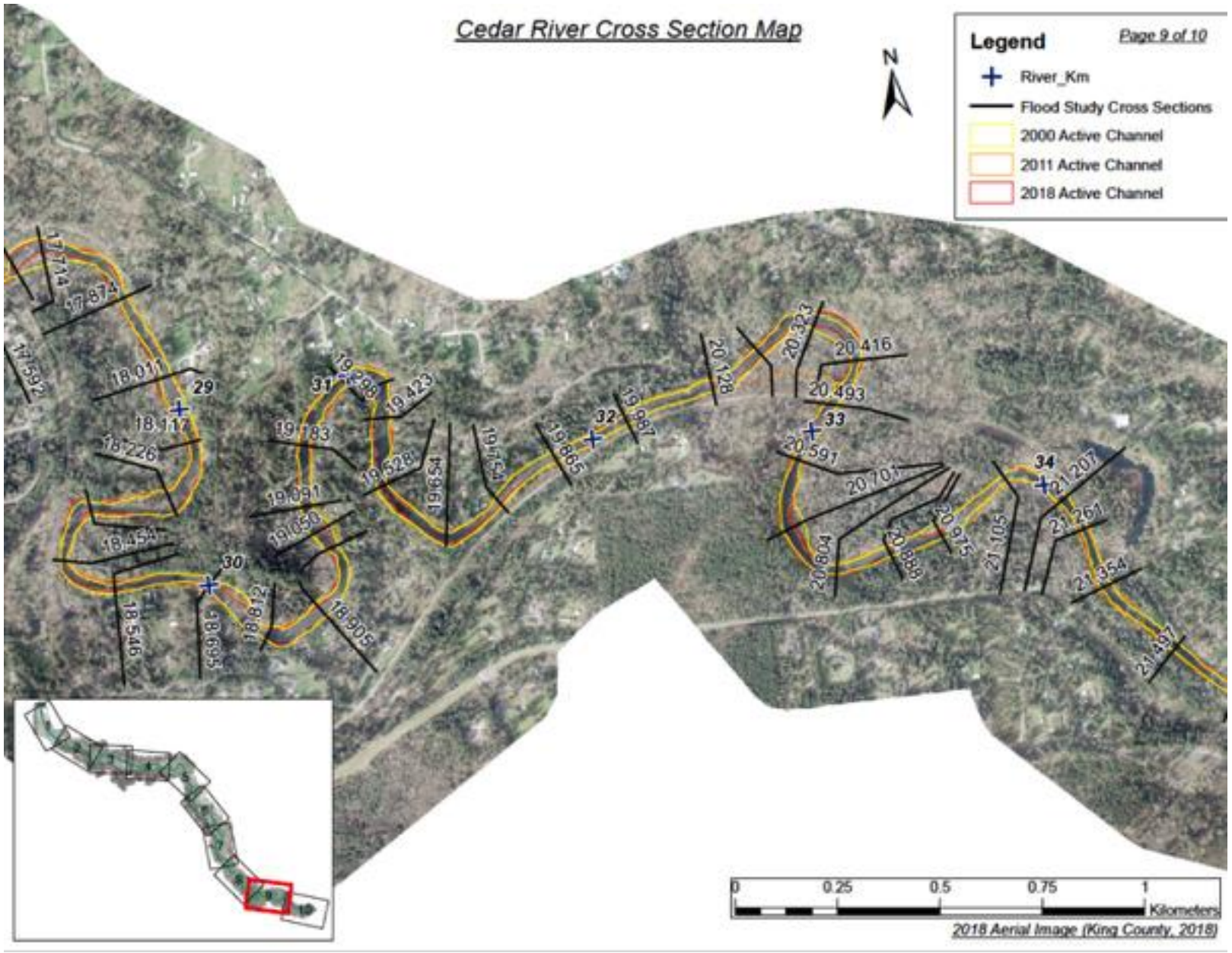
Cedar River Cross Section Map
Page 9 of 10
N
Legend
River_Km
Flood Study Cross Sections
2000 Active Channel
2011 Active Channel
2018 Active Channel
29
30
31
32
33
34
0
0.25
0.5
0.75
1
Kilometers
2018 Aerial Image (King County, 2018)

Cedar River Cross Section Map